

EPA/600/R-05/103  
August 2005

# **Organophosphate Pesticide Degradation Under Drinking Water Treatment Conditions**

By

Stephen E. Duirk and Timothy W. Collette  
National Exposure Research Laboratory  
Ecosystems Research Division  
Athens, GA

U.S. Environmental Protection Agency  
Office of Research and Development  
Washington D.C. 20460

## **NOTICE**

The information in this document has been funded by the United States Environmental Protection Agency. It has been subject to the Agency's peer and administrative review, and it has been approved for publication as an EPA document. Mention of trade names of commercial products does not constitute endorsement or recommendation for use.

## ABSTRACT

Chlorpyrifos (CP) was used as a model compound to develop experimental methods and prototype modeling tools to forecast the fate of organophosphate (OP) pesticides under drinking water treatment conditions. CP was found to rapidly oxidize to chlorpyrifos oxon (CPO) in the presence of free chlorine. The primary oxidant is hypochlorous acid (HOCl); thus, oxidation is more rapid at lower pH (i.e., below the  $pK_a$  of HOCl at 7.5). At elevated pH, both CP and CPO are susceptible to alkaline hydrolysis and degrade to 3,5,6-trichloro-2-pyridinol (TCP), a stable end product. Furthermore, the hydrolysis of both CP and CPO to TCP was shown to be accelerated in the presence of free chlorine by  $OCl^-$ . These observations regarding oxidation and hydrolysis are relevant to common drinking water treatment processes: disinfection and water softening, respectively. In this work, intrinsic rate constants for these processes were determined, and simple computer models have been developed that accurately predict the concentration of CP, CPO, and TCP as a function of pH, chlorine dose, CP concentration, and time after chlorine dosing. These models serve as a first step toward the development of tools to assess the assessment of risk associated with consuming treated drinking water whose source is contaminated with OP pesticides.

## FOREWORD

The National Exposure Research Laboratory Ecosystems Research Division (ERD) in Athens, Georgia, conducts process, modeling, and field research to assess the exposure risks of humans and ecosystems to both chemical and non-chemical stressors. This research provides data, modeling tools, and technical support to EPA Program and Regional Offices, state and local governments, and other customers, enabling achievement of Agency and ORD strategic goals for the protection of human health and the environment.

ERD research includes studies of the behavior of contaminants, nutrients, and biota in environmental systems, and the development of mathematical models to assess the response of aquatic systems, watersheds, and landscapes to stresses from natural and anthropogenic sources. ERD field and laboratory studies support process research, model development, testing and validation, and the characterization of variability and prediction uncertainty. Leading-edge computational technologies are developed to integrate core science research results into modeling systems that provide predictive capabilities for complex environmental exposure scenarios faced by the Agency.

This research project seeks to provide evaluated methods, tools, and databases for forecasting the fate of pesticides and other toxic chemicals in drinking water treatment systems. These products will be useful to EPA Program Offices and others who must evaluate the ultimate fate of chemicals that occur in drinking water sources. This report describes the development and testing of experimental methods and computational models to characterize and simulate chlorination and hydrolysis of organophosphate pesticides under drinking water treatment conditions. Chlorpyrifos and its degradates were used as model compounds for the study. This work is the first step in developing screening-level tools for forecasting chemical transformations in drinking water treatment scenarios, that ultimately will make assessment of risk from consuming drinking water more accurate.

Eric J. Weber, Ph.D.  
Director  
Ecosystems Research Division  
Athens, Georgia

## **ACKNOWLEDGEMENT**

The authors would like to thank Jimmy Avants and Chris Tarr for their technical assistance.

Also, we would like to thank Dr. Wayne Garrison, Dr. Jackson Ellington, Dr. Dan Cherney, and Dr. John Kenneke for their consultation and expertise.

## TABLE OF CONTENTS

TABLE OF CONTENTS.....	i
LIST OF TABLES.....	ii
LIST OF FIGURES.....	iii
EXECUTIVE SUMMARY.....	vi
1 INTRODUCTION.....	1
2 EXPERIMENTAL PROCEDURES.....	5
2.1 Materials.....	5
2.2 Methods.....	5
3 RESULTS AND DISCUSSION.....	9
3.1 Chlorpyrifos Reaction Order and Apparent Rate Constants.....	9
3.2 Degradation Pathways of Chlorpyrifos Oxon.....	10
3.3 Model Development.....	12
4 CONCLUSIONS.....	15
5 REFERENCES.....	18
TABLES.....	20
FIGURES.....	22

**LIST OF TABLES**

Table 1 Stoichiometric equations and rate coefficients used in the chlorpyrifos degradation pathway model. Numbers in parenthesis are 95% confidence intervals for the rate coefficients determined in this study. .... 21

## LIST OF FIGURES

Figure 1	Free chlorine loss in the presence of CP at pH 8.5. $[CP]_o = 0.5 \mu\text{M}$ , $[\text{CO}_3]_T = 10 \text{ mM}$ , Temperature = 25 °C, and $[\text{HOCl}]_T = 10, 50, 100 \mu\text{M}$ .	23
Figure 2	Free chlorine loss in the presence of CP at pH 9. $[CP]_o = 0.5 \mu\text{M}$ , $[\text{CO}_3]_T = 10 \text{ mM}$ , Temperature = 25 °C, and $[\text{HOCl}]_T = 10, 50, 100 \mu\text{M}$ .	24
Figure 3	Free chlorine loss in the presence of CP at pH 10. $[CP]_o = 0.5 \mu\text{M}$ , $[\text{CO}_3]_T = 10 \text{ mM}$ , Temperature = 25 °C, and $[\text{HOCl}]_T = 10, 50, 100 \mu\text{M}$ .	25
Figure 4	Free chlorine loss in the presence of CP at pH 11. $[CP]_o = 0.5 \mu\text{M}$ , $[\text{CO}_3]_T = 10 \text{ mM}$ , Temperature = 25 °C, and $[\text{HOCl}]_T = 10, 50, 100 \mu\text{M}$ .	26
Figure 5	Observed first order loss of CP as a function of free chlorine at pH 6.36. $[CP]_o = 0.5 \mu\text{M}$ , $[\text{PO}_4]_T = 10 \text{ mM}$ , Temperature = 25 °C, and $[\text{HOCl}]_T = 10, 50, 100 \mu\text{M}$ .	27
Figure 6	Observed first order loss of CP as a function of free chlorine at pH 7.5. $[CP]_o = 0.5 \mu\text{M}$ , $[\text{PO}_4]_T = 10 \text{ mM}$ , Temperature = 25 °C, and $[\text{HOCl}]_T = 10, 50, 100 \mu\text{M}$ .	28
Figure 7	Observed first order loss of CP as a function of free chlorine at pH 8.5. $[CP]_o = 0.5 \mu\text{M}$ , $[\text{CO}_3]_T = 10 \text{ mM}$ , Temperature = 25 °C, and $[\text{HOCl}]_T = 10, 50, 100 \mu\text{M}$ .	29
Figure 8	Observed first order loss of CP as a function of free chlorine at pH 8.75. $[CP]_o = 0.5 \mu\text{M}$ , $[\text{CO}_3]_T = 10 \text{ mM}$ , Temperature = 25 °C, and $[\text{HOCl}]_T = 10, 50, 100 \mu\text{M}$ .	30
Figure 9	Observed first order loss of CP as a function of free chlorine at pH 9. $[CP]_o = 0.5 \mu\text{M}$ , $[\text{CO}_3]_T = 10 \text{ mM}$ , Temperature = 25 °C, and $[\text{HOCl}]_T = 10, 50, 100 \mu\text{M}$ .	31
Figure 10	Observed first order loss of CP as a function of free chlorine at pH 10. $[CP]_o = 0.5 \mu\text{M}$ , $[\text{CO}_3]_T = 10 \text{ mM}$ , Temperature = 25 °C, and $[\text{HOCl}]_T = 10, 50, 100 \mu\text{M}$ .	32
Figure 11	Observed first order loss of CP as a function of free chlorine at pH 11. $[CP]_o = 0.5 \mu\text{M}$ , $[\text{CO}_3]_T = 10 \text{ mM}$ , Temperature = 25 °C, and $[\text{HOCl}]_T = 10, 50, 100 \mu\text{M}$ .	33
Figure 12	Reaction order of free chlorine with CP at pH 8.5. $[CP]_o = 0.5 \mu\text{M}$ , $[\text{CO}_3]_T = 10 \text{ mM}$ , Temperature = 25 °C, and $[\text{HOCl}]_T = 10, 50, 100 \mu\text{M}$ .	34
Figure 13	Reaction order of free chlorine with CP at pH 9.0. $[CP]_o = 0.5 \mu\text{M}$ , $[\text{CO}_3]_T = 10 \text{ mM}$ , Temperature = 25 °C, and $[\text{HOCl}]_T = 10, 50, 100 \mu\text{M}$ .	35
Figure 14	Reaction order of free chlorine with CP at pH 10. $[CP]_o = 0.5 \mu\text{M}$ , $[\text{CO}_3]_T = 10 \text{ mM}$ , Temperature = 25 °C, and $[\text{HOCl}]_T = 10, 50, 100 \mu\text{M}$ .	36



Figure 15 Reaction order of free chlorine with CP at pH 11.  $[CP]_o = 0.5 \mu\text{M}$ ,  $[\text{CO}_3]_T = 10 \text{ mM}$ , Temperature =  $25^\circ\text{C}$ , and  $[\text{HOCl}]_T = 10, 50, 100 \mu\text{M}$ . ..... 37

Figure 16 Apparent second order reaction rate coefficient for CP in the presence of free chlorine at pH 6.36.  $[CP]_o = 0.5 \mu\text{M}$ ,  $[\text{PO}_4]_T = 10 \text{ mM}$ , Temperature =  $25^\circ\text{C}$ , and  $[\text{HOCl}]_T = 10, 50, 100 \mu\text{M}$ . 95% confidence intervals about the regression line shown. .... 38

Figure 17 Apparent second order reaction rate coefficient for CP in the presence of free chlorine at pH 7.5.  $[CP]_o = 0.5 \mu\text{M}$ ,  $[\text{PO}_4]_T = 10 \text{ mM}$ , Temperature =  $25^\circ\text{C}$ , and  $[\text{HOCl}]_T = 10, 50, 100 \mu\text{M}$ . 95% confidence intervals about the regression line shown. .... 39

Figure 18 Apparent second order reaction rate coefficient for CP in the presence of free chlorine at pH 8.5.  $[CP]_o = 0.5 \mu\text{M}$ ,  $[\text{PO}_4]_T = 10 \text{ mM}$ , Temperature =  $25^\circ\text{C}$ , and  $[\text{HOCl}]_T = 10, 50, 100 \mu\text{M}$ . 95% confidence intervals about the regression line shown. .... 40

Figure 19 Apparent second order reaction rate coefficient for CP in the presence of free chlorine at pH 8.75.  $[CP]_o = 0.5 \mu\text{M}$ ,  $[\text{CO}_3]_T = 10 \text{ mM}$ , Temperature =  $25^\circ\text{C}$ , and  $[\text{HOCl}]_T = 10, 50, 100 \mu\text{M}$ . 95% confidence intervals about the regression line shown. .... 41

Figure 20 Apparent second order reaction rate coefficient for CP in the presence of free chlorine at pH 9.  $[CP]_o = 0.5 \mu\text{M}$ ,  $[\text{CO}_3]_T = 10 \text{ mM}$ , Temperature =  $25^\circ\text{C}$ , and  $[\text{HOCl}]_T = 10, 50, 100 \mu\text{M}$ . 95% confidence intervals about the regression line shown. .... 42

Figure 21 Apparent second order reaction rate coefficient for CP in the presence of free chlorine at pH 10.  $[CP]_o = 0.5 \mu\text{M}$ ,  $[\text{CO}_3]_T = 10 \text{ mM}$ , Temperature =  $25^\circ\text{C}$ , and  $[\text{HOCl}]_T = 10, 50, 100 \mu\text{M}$ . 95% confidence intervals about the regression line shown. .... 43

Figure 22 Apparent second order reaction rate coefficient for CP in the presence of free chlorine at pH 11.  $[CP]_o = 0.5 \mu\text{M}$ ,  $[\text{CO}_3]_T = 10 \text{ mM}$ , Temperature =  $25^\circ\text{C}$ , and  $[\text{HOCl}]_T = 10, 50, 100 \mu\text{M}$ . 95% confidence intervals about the regression line shown. .... 44

Figure 23 The pH dependence of the apparent second order rate constant for the reaction of free chlorine with CP.  $[CP]_o = 0.5 \mu\text{M}$ ,  $[\text{Buffer}]_T = 10 \text{ mM}$ , Temperature =  $25 \pm 1^\circ\text{C}$ , and  $[\text{HOCl}]_T = 10, 50, \text{ and } 100 \mu\text{M}$ . Error bars represent 95% confidence intervals. .... 45

Figure 24 Experimental and model predictions for the first order observed hydrolysis of CPO over the pH range of 1-11.  $[\text{CPO}]_o = 0.5 \mu\text{M}$ ,  $[\text{Buffer}]_T = 10 \text{ mM}$ , and Temperature =  $25 \pm 1^\circ\text{C}$ ,. Error bars represent 95% confidence intervals and the line represents model results..... 46

Figure 25 Second order rate coefficient for chlorine assisted hydrolysis of CPO at pH 9 and 10.9.  $[\text{CPO}]_o = 0.5 \mu\text{M}$ ,  $[\text{CO}_3]_T = 10 \text{ mM}$ , Temperature =  $25 \pm 1^\circ\text{C}$ , and  $[\text{HOCl}]_T = 0 - 250 \mu\text{M}$ . Error bars represent 95% confidence intervals. .... 47

Figure 26 Simplified schematic of chlorpyrifos degradation pathways in the presence of chlorine at near neutral and alkaline pH. .... 48

Figure 27 TCP experimental and model results for the loss of CP in the presence of free chlorine at pH 11 .  $[CP]_0 = 0.35 \mu\text{M}$ ,  $[\text{CO}_3]_{\text{T}} = 10 \text{ mM}$ , Temperature =  $25 \pm 1^\circ\text{C}$ , and  $[\text{HOCl}]_{\text{T}} = 0 - 150 \mu\text{M}$ . Lines represent model results. .... 49

Figure 28 CP degradation in the presence of free chlorine at pH 7.15.  $[CP]_0 = 0.33 \mu\text{M}$ ,  $[\text{CO}_3]_{\text{T}} = 1 \text{ mM}$ , Temperature =  $25 \pm 1^\circ\text{C}$ , and  $[\text{HOCl}]_{\text{T}} = 20 \mu\text{M}$ . Lines represent model results and error bars are 95% confidence intervals..... 50

Figure 29 CP degradation in the presence of free chlorine at pH 9.0.  $[CP]_0 = 0.5 \mu\text{M}$ ,  $[\text{CO}_3]_{\text{T}} = 1 \text{ mM}$ , Temperature =  $25 \pm 1^\circ\text{C}$ , and  $[\text{HOCl}]_{\text{T}} = 10 \mu\text{M}$ . Lines represent model results and error bars are 95% confidence intervals. .... 51

## EXECUTIVE SUMMARY

Environmental regulations require that all relevant routes of human consumption be considered in risk assessments for anthropogenic chemicals. A large percentage of the US population consumes drinking water (DW) that is treated. There is available monitoring data for important pesticides and toxic chemicals in DW sources (both surface and ground water). However, there is very little monitoring data for these chemicals or their degradates in finished DW. Limited experimental studies show that some chemicals are partially removed by physical water treatment processes (e.g., filtration, flocculation, etc.), and some are transformed by reactions that occur during chemical treatment (e.g., disinfection and softening). Transformations of some contaminants have been shown to produce products that are more toxic than the parent compound.

This report is in partial fulfillment of the National Exposure Research Laboratory Task # 16608, “Fate of Pesticides and Toxic Chemicals During Drinking Water Treatment”, under Goal 4, GPRA Objective 4.5, and GPRA Sub-objective 4.5.2. The goals of this research task are to: 1) provide chemical-specific information on the effects of water treatment for high-priority pollutants, 2) provide physicochemical parameters for transformation products, and 3) develop predictive models for forecasting treatment effects that cross chemical class and treatment conditions. Toward this end, the efforts described in this report provide evaluated information on the chemical transformations of chlorpyrifos (CP), a widely used organophosphate (OP) pesticide, under drinking water treatment conditions. In addition, this report describes the first steps toward developing predictive models for forecasting chemical treatment effects for the entire class of OP pesticides.

For this effort, the loss of CP in the presence of free chlorine in laboratory-prepared aqueous solution was observed. This loss was found to be first order with respect to both CP concentration and to free chlorine concentration. A total of two transformation products were observed with near-complete mass balance – chlorpyrifos oxon (CPO) and 3,5,6-trichloro-2-pyridinol (TCP). The transformation of CP to CPO occurs via oxidation by hypochlorous acid (HOCl). This reaction is rapid, and increasingly so as pH decreases due to the  $pK_a$  of HOCl at 7.5. This observation is relevant for drinking water disinfection, which is often achieved using chlorine near neutral pH. The oxon degradates of OP pesticides are typically much more toxic than the parent compound.

Both CP and CPO were observed to hydrolyze to TCP, particularly at higher pH. The most prominent form of hydrolysis is base-catalyzed. Also, for the first time, we report here a transformation pathway of hydrolysis for both CPO and CP that is assisted by  $OCl^-$  when chlorine is present under alkaline conditions. These observations are relevant for drinking water softening, which is often achieved by significantly raising the pH (by adding lime or soda ash) in order to precipitate minerals. Hydrolysis products such as TCP are generally less toxic than the parent OP pesticides.

Results of the experiments described herein demonstrate that the change in risk (associated with anthropogenic chemicals in source waters) due to DW treatment is a complex issue. For example, while oxidation of OP pesticides by chlorine below neutral pH leads very rapidly to a more toxic form, hydrolysis (assisted by chlorine) above neutral pH leads to a less toxic form. Because of this complexity, we have chosen to develop screening-level models that forecast the concentrations of all reaction products as a function of pH, chlorine dose, OP pesticide concentration, and time after chlorine dosing. To test this approach, we have

determined intrinsic rate constants for all relevant pathways of transformation for CP in chlorinated water. Using these simple models and intrinsic rate constants, we demonstrate that the concentrations of CP, CPO, and TCP can be adequately described under a variety of scenarios that are similar to DW treatment conditions.

The work reported here serves as the first steps – and the “proof-of-concept” – towards the development of a comprehensive modeling tool for OP fate in drinking water treatment plants and distribution systems. Following the reported work, we have now begun to apply the experiments and models to other OP pesticides that were judiciously selected to reflect the full range of chemical structure variability in this class. Our objective is to develop predictive models that associate relative rates of reactivity to structural variability. This will allow decision makers to rank and prioritize chemicals found in drinking water sources according to potential risk. Also, we are currently in the process of identifying natural aqueous matrix components that most significantly affect the rates and pathways of transformation of anthropogenic chemicals under DW treatment conditions. For example, we are evaluating the impacts of natural organic matter (NOM) and bromide ion concentration on the oxidation of CP. NOM can serve as a “sink” (or “demand”) for free chlorine and reduce the observed rate of oxidation. On the other hand, bromide can be oxidized by chlorine to form hypobromous acid, which is a more potent oxidant than hypochlorous acid. Therefore, the presence of bromide can increase the observed oxidation of CP. The goal of these experiments is to incorporate these most-important matrix effects into our models so that the models can be applied to actual DW treatment scenarios.

## 1 INTRODUCTION

Numerous drinking water sources have been contaminated with pesticides, pharmaceuticals, plasticizers, antimicrobial agents, as well as many other potentially harmful chemicals.<sup>1,2</sup> The fate for many of these compounds under drinking water treatment conditions is a concern due to the potential adverse health effects by consuming contaminated potable water. Physical surface water treatment processes (coagulation/flocculation, sedimentation, and filtration) do not appear to remove or transform most hydrophilic chemicals.<sup>3</sup> On the other hand, chlorine has been shown to transform some of these chemicals.<sup>4-7</sup> However, few studies have included a thorough investigation of the ultimate fate of these transformation products.

The Food Quality Protection Act of 1996 (FQPA) requires that all pesticide chemical residuals in or on food be considered for anticipated exposure. Drinking water is considered a potential pathway for dietary exposure, but there is reliable monitoring data for only the source water. For example, the United States Geological Survey (USGS) completed a national reconnaissance survey known as NAWQA (National Water Quality Assessment) to help define human exposure to various contaminants.<sup>8</sup> For the NAWQA survey, 90 pesticides (and some selected metabolites) were chosen as target chemicals to monitor in US drinking water sources. However, there is a relative dearth of information on occurrence of pesticide residuals and pesticide metabolites in finished drinking water. Two surveys have been conducted for a few community water systems examining pesticide concentrations in the source and finished drinking water.<sup>9,10</sup> Neither of these studies thoroughly examined the effect of each treatment process on a single slug of water, hence only the influent and effluent of each treatment facility could be qualitatively discussed with respect to overall removal efficacy. Also, these studies did not account for the treatment plant hydraulic retention time, thus it was not possible to ensure that

influent and effluent samples were properly paired. Clearly, more thorough occurrence studies that include monitoring drinking water for both pesticides and their expected transformation products are needed.

Chlorination is the most commonly used chemical disinfectant for community water systems<sup>11</sup> and is known to react with numerous pesticides. For example, four s-triazines were found to degrade in the presence of free chlorine ( $\text{HOCl} + \text{OCl}^-$ ).<sup>12,13</sup> The proposed reaction center and transformation pathway for each s-triazine was oxidation of the sulfur resulting in the formation of sulfoxide and sulfone degradation products. Atrazine was also found to be significantly degraded by ozone;<sup>14</sup> however, subsequent chlorination of the ozonated effluent had very little affect on concentration of residual atrazine or its ozone degradation products.<sup>9</sup>

Some carbamate pesticides have been shown to react with free chlorine while other members of this pesticide class were found to be stable in chlorinated water. For example, carbaryl and propoxur do not react with free chlorine; but, aldicarb, methomyl, and thiobencarb do exhibit significant reactivity.<sup>15-17</sup> The sulfoxide degradate of thiobencarb – produced by reaction with free chlorine – was found to be mutagenic.<sup>17</sup> However, the by-products of aldicarb were found to be less toxic than the parent.<sup>15</sup> These findings demonstrate that free chlorine reactivity with different members in a specific class of pesticides can vary significantly due to chemical structure variations. Therefore, it is prudent to study the fate and transformation pathways of entire chemical classes, using class members that exhibit systematic structural variations and employing carefully selected experimentation and numerical modeling.

When chlorine reacts with the phosphorothioate subgroup of organophosphate (OP) pesticides, the thiophosphate functionality ( $\text{P}=\text{S}$ ) can be oxidized to its corresponding oxon ( $\text{P}=\text{O}$ ).<sup>18-20</sup> The resulting oxons are typically more potent than the parent as an inhibitor of

acetylcholinesterase, an enzyme necessary for proper function of the nervous system.<sup>20</sup> Margra et al.,<sup>19</sup> investigated the stability of diazoxon at neutral pH in the presence of chlorine and found that it was relatively stable after 48 hours (i.e., over 50% remained). Thus, it was assumed that the oxons are resistant to further oxidation by aqueous chlorine. However, the oxon form is more susceptible to neutral and alkaline hydrolysis than is the parent pesticide.<sup>21</sup> To our knowledge, no additional experiments have been conducted to determine the stability of oxons under conditions relevant to drinking water treatment.

As mentioned previously, twelve community water systems were recently surveyed for pesticide contamination in both their source and finished waters.<sup>10</sup> Three OP pesticides (diazinon, chlorpyrifos, and malathion) were commonly detected in the source water. However, the parent compounds were never detected in finished potable water. This suggests that the pesticides were completely eliminated by drinking water treatment, but this seems unlikely given that most hydrophilic chemicals are not significantly removed by physical treatment processes. On the other hand, this observation could mean that the parent OPs were completely transformed to the more toxic oxon forms, which were not target analytes in the surveys. The reaction rates and pathways of OP pesticide degradation under drinking water treatment conditions have yet been investigated fully enough to determine if such an assumption is warranted.

The purpose of this study reported herein was to further elucidate the kinetics and degradation pathways of OP pesticides in the presence of free chlorine. Chlorpyrifos (CP) was chosen as a model OP pesticide due to its widespread use and the frequency that it has been found in drinking water sources. The first-order observed rate constants were obtained for CP loss in the presence of increasing chlorine concentrations over the pH range of 6.3-11. The reaction orders for both CP and free chlorine were then determined. Then, from the apparent



second order rate coefficients, the intrinsic rate coefficient for hypochlorous acid (HOCl) reacting with CP was determined. Since the aqueous stability of chlorpyrifos oxon (CPO) was relatively unknown, hydrolysis experiments for CPO were conducted over the pH range of 1-11. Also, CPO stability in the presence of free chlorine was examined over the pH range of 4-11. These experiments resulted in elucidation of the degradation pathways for CP and CPO in the presence of free chlorine. A model was developed from the proposed degradation pathways that is capable of temporally predicting the loss of CP and CPO as well as the formation of 3,5,6-trichloro-2-pyridinol (TCP), which is the final degradate for these reactions.

## 2 EXPERIMENTAL PROCEDURES

### 2.1 *Materials*

Chlorpyrifos (99.5%), chlorpyrifos oxon (98.7%), and 3,5,6-trichloro-2-pyridinol (99%) were purchased from ChemService (West Chester, PA). Commercial 10-13% sodium hypochlorite (NaOCl), purchased from Aldrich (Milwaukee, WI), contained equimolar amounts of OCl<sup>-</sup> and Cl<sup>-</sup>. Aqueous stock solutions and experiments utilized laboratory-prepared deionized water (18 MΩ cm<sup>-1</sup>) from a Barnstead ROPure Infinity™/NANOPure™ system (Barnstead-Thermolyne Corp., Dubuque, IA). Phosphate and carbonate salts used for buffer solutions were dissolved in deionized water and filtered through a 0.45 μm filter, which was pre-rinsed with deionized water. The pH for the experiments was adjusted with either 1 N H<sub>2</sub>SO<sub>4</sub> or NaOH. All organic and inorganic chemicals were certified ACS reagent grade and used without further purification.

### 2.2 *Methods*

The glassware and polytetrafluoroethylene (PTFE) septa used in this study were soaked in a concentrated free chlorine solution for 24 hours, rinsed with deionized water, and dried at 105 °C prior to use. All pH measurements were obtained using an Orion 940 pH meter with a Ross combination electrode from Fisher Scientific (Pittsburgh, PA). All chlorination and hydrolysis experiments were conducted at constant temperature (25±1°C). All kinetic experiments used to estimate rate coefficients measured at least 87% loss in parent compound.

For all CP oxidation experiments, CP was spiked by adding 1 mL of 4 mM stock in ethyl acetate into an empty 4 L borosilicate glass Erlenmeyer flask. A gentle flow of nitrogen gas was used to evaporate the ethyl acetate and 4 L of deionized water was then added to the flask. The solution was slowly stirred and allowed to dissolve for 12 hours resulting in an aqueous concentration of 1  $\mu\text{M}$ . CP chlorination kinetic experiments were conducted under pseudo-first-order conditions, total chlorine to chlorpyrifos molar ratios of 20:1, 100:1, and 200:1. Chlorine was added to solutions under rapid mix conditions achieved with a magnetic stir plate and a PTFE-coated stir bar. At each discrete sampling interval, two reaction vessels were sacrificed in their entirety. One vessel was used to determine total free chlorine concentration ( $[\text{HOCl}]_{\text{T}} = [\text{HOCl}] + [\text{OCl}^-]$ ) via Standard Method 4500-Cl F DPD-FAS titrimetric method.<sup>22</sup> In the other vessel, free chlorine residuals were quenched with sodium sulfite in 20% excess of the initial free chlorine concentration. The pH of a 100 mL aliquot was then adjusted to 2 for analysis of CP and its degradation products.

Above pH 8, 10 mM carbonate  $[\text{CO}_3]_{\text{T}}$  buffer was used to maintain pH. The purchased free chlorine solution was first diluted to 18,000 mg- $\text{Cl}_2/\text{L}$ . The diluted free chlorine stock solution was added to the aqueous system containing 0.5  $\mu\text{M}$  chlorpyrifos and 10 mM carbonate buffer in a 2 L Erlenmeyer flask. After mixing, thirteen aliquots from the large 2 L reactor were placed into 128 mL amber reaction vessels with PTFE septa and stored in a water bath at  $25 \pm 1^\circ\text{C}$  in the dark.

In the pH range of 6.0-7.5, the rate of CP loss in the presence of free chlorine was very fast. Therefore, twelve 100 mL aliquots from a 2 L aqueous system containing 10 mM phosphate buffer,  $[\text{PO}_4]_{\text{T}}$ , and 0.5  $\mu\text{M}$  CP were placed in 250 mL amber Erlenmeyer flasks. Each individual reaction vessel was brought up to  $25 \pm 1^\circ\text{C}$  via water bath immersion. Free

chlorine was then added to each reactor while under rapid mix conditions with a magnetic stir plate and PTFE-coated stir bar. The reaction vessels were then re-immersed in the water bath. At designated time intervals, reactors were quenched with 20% excess stoichiometric sodium sulfite compared to the initial free chlorine concentration and CP and its degradation products were extracted. The time frame of these experiments was under 1 hour. Parallel experiments were conducted to determine free chlorine concentrations as a function of time.

The reactivity of free chlorine with CPO was also examined. The experimental procedures were the same as for CP in the presence of free chlorine above pH 8. Since there is a lack of CPO hydrolysis rate coefficients in the literature, hydrolysis experiments in the absence of free chlorine were also conducted over the pH range of 1 to 11.

Additionally, model validation experiments were conducted at pH 7.1 and 9.0. These experiments were conducted in triplicate via the procedures outlined previously for CP oxidation experiments above pH 8. Experimental conditions were chosen to reflect drinking water treatment conditions:  $[\text{CO}_3]_{\text{T}} = 1.0 \text{ mM}$  and  $[\text{HOCl}]_{\text{T}} = 20$  and  $10 \text{ }\mu\text{M}$  at pH 7.1 and 9 respectively.

CP and its degradation products were extracted from water using C-18 solid phase extraction (SPE) cartridges purchased from Supleco (Bellefonte, PA). First, the pH of a 100 mL sample was adjusted to  $\text{pH} \leq 2$  to increase the recovery of TCP ( $\text{pK}_a = 4.55$ ) on the solid phase adsorbent.<sup>23</sup> Then, the sample was spiked with  $1 \text{ }\mu\text{M}$  of phenthorate (internal standard), mixed thoroughly by hand for two minutes, passed through the SPE cartridge at an approximate flow-rate of  $7 \text{ mL/min}$ , and eluted with  $3 \text{ mL}$  of ethyl acetate. Quantification for each analyte was compared to eight extracted standards over the concentration range of  $0.01$  to  $1 \text{ }\mu\text{M}$ . A Hewlett-Packard 6890 GC equipped with a 5973 MSD was used to analyze CP, CPO, and TCP. GC

## OP Pesticide Degradation under DW Conditions

conditions were as follows: 30-m Restek Rtx-200 column with a 0.25-mm ID and 0.5- $\mu$ m film thickness. The temperature profile was: 100 °C for 5 minutes, 100 to 250 °C at 10 °C/minute, and then held at 250 °C for 25 minutes. Mass balances of 80% or greater were obtained for each experiment.

### 3 RESULTS AND DISCUSSION

#### 3.1 *Chlorpyrifos Reaction Order and Apparent Rate Constants*

The observed loss of CP in the presence of free chlorine was initially assumed to be first order with respect to CP concentration. If linearity is observed when plotting  $\ln([CP]/[CP]_0)$  versus time (t), then this assumption would be valid when free chlorine is present in excess. (Note that  $[CP]/[CP]_0$  is the measured concentration of CP at a discrete sampling time divided by the initial concentration of CP.) The slope of the regression line from such a plot yields the observed first order rate coefficient ( $k_{\text{obs}}$ ) for CP loss as described by the following rate expression:

$$\ln \frac{[CP]}{[CP]_0} = -k_{\text{obs}} t \quad (1)$$

Prior to examining plots of  $\ln([CP]/[CP]_0)$  versus t, we established, as shown in Figures 1 – 4, that free chlorine was in excess and that the concentration of free chlorine did not change significantly over the course of the reactions. Then, we generated plots of  $\ln([CP]/[CP]_0)$  versus t at a variety of pHs and for different concentrations of free chlorine. As demonstrated in Figures 5 – 11, CP exhibited first order dependency with respect to itself when reacting in the presence of free chlorine under these experimental conditions. For example, Figure 7 shows the first order observed loss of CP at pH 8.5 and  $[HOCl]_T = 10, 50, \text{ and } 100 \mu\text{M}$ . The first order rate coefficients for the various experimental conditions were determined from the slopes of the regression lines displayed in Figures 5 – 11.

Next, we determined the order of the reaction with respect to free chlorine at the various pHs by plotting the log of the observed first order rate coefficients versus the log of the initial

free chlorine concentrations (Figures 12 – 15). The slope of the regression lines in these figures indicate the reaction order with respect to total free chlorine was approximately 1 over the entire pH range sampled. For example, as demonstrated in Figure 12, at pH 8.5 the slope was found to be 1.103 with an  $r^2$  of 0.998.

The second order apparent rate coefficient ( $k_{app}$ ) at each pH was determined by plotting  $k_{obs}$  versus the initial free chlorine concentration. Since both species of free chlorine are present ( $\text{HOCl} + \text{OCl}^-$ ), the apparent second order loss of CP in the presence of free chlorine can be described as

$$k_{obs} = k_{app} [\text{HOCl}]_T \quad (2)$$

$$\frac{d[\text{CP}]}{dt} = -k_{app} [\text{HOCl}]_T [\text{CP}] \quad (3)$$

Figures 16 – 22 show that, for all pH  $k_{obs}$  increases linearly with increasing free chlorine concentration. This indicates that the observed first order rate coefficients are proportional with increasing free chlorine concentration for each pH examined. In addition,  $k_{app}$  (calculated from equation 2) increased as pH decreased from 11 to 6.3 (Figure 23). The  $pK_a$  of hypochlorous acid ( $\text{HOCl}$ ) is 7.5.<sup>24</sup> If the dominant reacting species is  $\text{HOCl}$ , then the apparent rate coefficient should increase as pH decreases.

### 3.2 *Degradation Pathways of Chlorpyrifos Oxon*

Due to the fact that diazoxon was resistant to further oxidation by free chlorine,<sup>19</sup> disappearance of CPO in the presence of free chlorine was assumed to only occur via alkaline hydrolysis. Unlike CP,<sup>25</sup> there has been no thorough examination of CPO hydrolysis. It was thought that CPO would behave similarly to CP except the oxon hydrolysis rate would be faster,

as has been seen with other OP pesticides and their oxon analogues.<sup>21</sup> The hydrolytic behavior of CPO in the absence of chlorine was found in the study reported here (Figure 24) to be similar to that found previously for CP. Both CPO and CP do not have an acid assisted component to the observed first order hydrolytic loss. Over the pH range of 1-7, the neutral hydrolysis component was found to be:  $k_{N,CPO} = 2.19 \times 10^{-3} \pm 1.73 \times 10^{-3} \text{ h}^{-1}$ . This is an order of magnitude faster than the neutral hydrolysis component previously reported for CP.<sup>25</sup> The alkaline hydrolysis rate coefficient ( $k_{B,CPO}$ ) was determined by plotting the observed first order loss of CPO versus the hydroxide ion concentration over the pH range of 8.5-11. The slope of the regression line yielded the alkaline hydrolysis rate coefficient:  $k_{B,CPO} = 229.2 \pm 18.7 \text{ M}^{-1}\text{h}^{-1}$ . Half-lives for CPO at pH 9, 10, and 11 were 80.5, 17.7, and 2.8 hours respectively. In Figure 24, the first order observed rate coefficients for CPO were adequately predicted using the neutral and alkaline assisted hydrolysis rate coefficients. Alkaline hydrolysis appears to be the only relevant CPO hydrolysis pathway under drinking water treatment conditions in the absence of chlorine.

The stability of CPO in the presence of free chlorine over the pH range of 4-11 was also investigated. Over the pH range pH 4-7, less than 1% of CPO was lost over a period of 6 hours in the presence of 100  $\mu\text{M}$  free chlorine. These experiments established that CPO is not susceptible to further oxidation since they were conducted below the  $\text{pK}_a$  of HOCl, which is a stronger oxidant than  $\text{OCl}^-$ . However, the first order observed loss of CPO increased linearly with increasing free chlorine concentration from 0-250  $\mu\text{M}$  at both pH 9 and 10.9 (Figure 25). The only detected transformation product was TCP at greater than 80% mass balance for all experiments. The regression lines in Figure 25 were found to be parallel and the slope of each line was an order of magnitude greater than the rate coefficient determined for alkaline hydrolysis ( $k_{B,CPO}$ ) in the absence of chlorine. These results suggest the presence of an  $\text{OCl}^-$



assisted hydrolysis pathway. For example,  $\text{OCl}^-$  could be serving as a nucleophile similar to  $\text{OH}^-$  in the alkaline hydrolysis process. It could then be proposed that CP would also be susceptible to chlorine assisted hydrolysis. Chlorine assisted hydrolysis has been observed by others investigating the formation and degradation of dichloroacetonitrile, a disinfection by-product (DBP), in the presence of chlorine and natural organic matter (NOM).<sup>26</sup>

### 3.3 Model Development

A kinetic model was developed to predict temporal concentrations of CP, CPO, and TCP. Figure 26 schematically shows the proposed degradation pathways for CP and CPO in the presence of free chlorine. This includes the observed pathways for which kinetic rate coefficients were experimentally determined. However, the intrinsic rate coefficients for hypochlorous acid and hypochlorite reacting with CP cannot be determined through direct experimental observation. The following set of ordinary differential equations (ODEs), based upon the presumed stoichiometric reactions in Table 1, were used to model the fate of CP and its degradates in the presence of free chlorine.

$$\frac{d[\text{CP}]}{dt} = -k_r[\text{HOCl}][\text{CP}] - k_{h,\text{CP}}[\text{CP}] - k_{\text{OCl},\text{CP}}[\text{OCl}^-][\text{CP}] \quad (4)$$

$$\frac{d[\text{CPO}]}{dt} = k_r[\text{HOCl}][\text{CP}] - k_{h,\text{CPO}}[\text{CPO}] - k_{\text{OCl},\text{CPO}}[\text{OCl}^-][\text{CPO}] \quad (5)$$

$$\frac{d[\text{TCP}]}{dt} = k_{h,\text{CP}}[\text{CP}] + k_{\text{OCl},\text{CP}}[\text{OCl}^-][\text{CP}] + k_{h,\text{CPO}}[\text{CPO}] + k_{\text{OCl},\text{CPO}}[\text{OCl}^-][\text{CPO}] \quad (6)$$

Equation 4 describes the loss of CP due to oxidation by hypochlorous acid, hydrolysis, and chlorine assisted hydrolysis. Equation 5 describes the formation of CPO as well as its loss by hydrolysis and chlorine assisted hydrolysis. TCP was found to be a stable end-product from the

loss of CP and CPO. Equation 6 incorporates all known and proposed TCP formation pathways, i.e., hydrolysis and chlorine assisted hydrolysis pathways for both CP and CPO.

Scientist™, an ODE solver by Micromath (Salt Lake City, UT), was used to fit the intrinsic rate coefficients for CP oxidation by hypochlorous acid ( $k_r$ ) and chlorine assisted hydrolysis of CP by hypochlorite ( $k_{\text{OCl,CP}}$ ), using non-linear regression analysis and the Powell algorithm solution method. The intrinsic rate coefficient ( $k_r$ ) was first fitted using the lower pH data, pH 6.3, because TCP formation was less than 0.025  $\mu\text{M}$  and approximately 93% of free chlorine was in the form of HOCl. Hence, hydrolysis of CP under these conditions could be largely neglected. The  $k_{\text{app}}$  at pH 6.3 was  $1.51 (\pm 0.26) \times 10^6 \text{ M}^{-1}\text{h}^{-1}$  (Figure 23) and the fitted value for  $k_r = 1.72 (\pm 0.68) \times 10^6 \text{ M}^{-1}\text{h}^{-1}$  (Table 1). (The numbers in parentheses are 95% confidence intervals.) The fitted value for  $k_r$  was expected to be slightly higher to account for the small amount of free chlorine in the hypochlorite form. Since the confidence intervals for  $k_{\text{app}}$  at pH 6.3 and  $k_r$  overlap, the intrinsic rate coefficient  $k_r$  can be approximated quite well from experiments conducted just below neutral pH. The intrinsic rate coefficient  $k_{\text{OCl,CP}}$  was fitted at pH 11 and  $[\text{HOCl}]_{\text{T}} = 0\text{-}150 \mu\text{M}$  (Figure 27). As the initial dose of free chlorine increased, TCP formation increased. While CPO was detected at  $[\text{HOCl}]_{\text{T}}$  equal to or greater than 50  $\mu\text{M}$ ,  $[\text{CPO}]$  never exceeded 0.025  $\mu\text{M}$  over the time course of the experiments. Using the fitted value for  $k_r$ , the value for  $k_{\text{OCl,CP}}$  was found to be  $990 (\pm 200) \text{ M}^{-1}\text{h}^{-1}$  (Table 1). The  $k_{\text{app}}$  for these experiments at pH 11 was  $2355 (\pm 859) \text{ M}^{-1}\text{h}^{-1}$ , which is more than twice the fitted value of  $k_{\text{OCl,CP}}$ . However, the  $k_{\text{app}}$  at pH 11 accounts for the total loss of CP including losses due to trace quantities of HOCl oxidizing CP to CPO. The  $k_r$  was found to be sufficiently large to describe the oxidation of CP over the pH range of 6.3-11, and  $k_{\text{OCl,CP}}$  was found to adequately describe chlorine assisted hydrolysis when the dominant form of free chlorine is OCl<sup>-</sup>.

Previous work with diazinon had proposed that hypochlorite participated in the formation of diazoxon<sup>18</sup>. This assumption was derived by plotting apparent second order rate coefficients versus hydrogen ion activity. The intercept of the plot was then interpreted as the intrinsic rate coefficient for hypochlorite reacting with diazinon at zero hydrogen ion activity. However, diazoxon was not measured in each experiment; therefore, the disappearance of diazinon in the presence of hypochlorite was assumed to be an oxidation reaction but was never confirmed. The intrinsic rate coefficient for hypochlorous acid ( $k_0$ ) was calculated based on the proportions of each chlorine species present at a given pH, the  $k_{app}$  with respect to experimental conditions, and the intrinsic rate coefficient for hypochlorite ( $k_1$ ) reaction with diazinon that was previously determined at zero hydrogen ion activity.

$$k_{app} = \alpha_0 k_0 + \alpha_1 k_1 \quad (7)$$

where  $\alpha_0$  and  $\alpha_1$  are the fractions of free chlorine that are present as hypochlorous acid and hypochlorite, respectively. The intrinsic rate coefficients for diazinon loss in the presence of free chlorine were:  $k_0 = 4.68 \times 10^5 \text{ M}^{-1}\text{h}^{-1}$  and  $k_1 = 972 \text{ M}^{-1}\text{h}^{-1}$ .<sup>18</sup> The experimental procedure was similar to the work presented here but only over the pH range of 9-11. Since experiments were not conducted near neutral pH,  $k_0$  may have been underestimated. However,  $k_1$  for diazinon loss was similar to our fitted rate coefficient for chlorine assisted hydrolysis of CP.

## 4 CONCLUSIONS

Experiments measuring CP loss in the presence of free chlorine identified degradation pathways based on mass balances over the pH range of 6.3-11. Hypochlorous acid was found to rapidly oxidize CP to CPO, and CP hydrolysis rate constants were obtained from literature. It was proposed that hypochlorite assists hydrolysis of CP, based on experimental observations of CPO hydrolysis in the presence of free chlorine at pH 9 and 10.9. Also, TCP was found to be a stable end-product for both CP and CPO degradation pathways in the presence of free chlorine.

Using the rate coefficients in Table 1, the proposed model was validated at pH 7.1 and 9 under conditions similar to drinking water treatment. At pH 7.1 and  $[\text{HOCl}]_{\text{T}} = 20 \mu\text{M}$  (Figure 28), almost all of the CP present was oxidized to CPO in 5 minutes. After 35 minutes, CP was no longer detected and CPO was the primary degradation product. Since CPO was found to be stable near neutral pH and  $100 \mu\text{M}$  free chlorine, the potential toxicity of the effluent could pose a greater risk to human health than if CP did not degrade.

At pH 9 and  $[\text{HOCl}]_{\text{T}} = 10 \mu\text{M}$  (Figure 29), CP loss was significantly slower than at pH 7.1. This was due both to the higher pH and lower chlorine dose. The predominant product after six hours was CPO; however, TCP concentrations were found to increase with time throughout the experiment. The increase in TCP concentration over the experimental time-frame is likely due to both ordinary alkaline hydrolysis and chlorine assisted hydrolysis.

Our computational model adequately predicted loss of CP, the formation and degradation of CPO, and the formation of TCP for both experimental conditions. This shows that CPO formation is controlled by the presence and availability of HOCl. Also, CPO stability is highly

pH dependent. These conditions were chosen to reflect water plant operating parameters and also to show that mechanistic models are robust and have the ability to predict degradation pathways under a variety of conditions.

The ability to model the fate and kinetics of a single compound (e.g., CP) under drinking water chlorination conditions has been established. Other recent papers have reported thorough studies of the degradation of surface water contaminants and model compounds in the presence of chlorine.<sup>4,6,27</sup> These studies included investigation of chlorination at relatively low pH, below 6, and found that the rate of disappearance of some pharmaceuticals, dihydroxybenzenes, and endocrine disruptors increased significantly compared to reactions at higher pH. We observed a similar phenomenon in experiments at pH below 6 with CP. To explain the significant increase in observed degradation rates, other researchers have proposed an acid catalyzed process resulting in the formation of  $\text{H}_2\text{OCl}^+$ . The  $\text{pK}_a$  of this species was approximated to be in the range of -3 to -4.<sup>28</sup>



The reaction rate coefficients for the  $\text{H}_2\text{OCl}^+$  species were calculated and found to be diffusion controlled for dihydroxybenzenes and endocrine disruptors, involving attack at the phenolic ring.<sup>6,27</sup> Wang and Margerum<sup>29</sup> theorized that a form similar to this species could exist in the transition state as part of the one-step acid catalyzed mechanism in the reversible hydrolysis of aqueous  $\text{Cl}_2$ . However, it is unclear if  $\text{H}_2\text{OCl}^+$  is the reacting species or  $\text{Cl}_{2(\text{aq})}$ . We are currently investigating this phenomenon for low pH oxidation of CP.

Mechanistic models greatly increase our understanding of the parameters controlling the rate of reactions for a specific compound. The ability to model degradation pathways of chemicals within a specific class still needs to be addressed. The research presented here is the

first step towards developing models to predict degradation pathways for the entire class of OP pesticides under more realistic drinking water treatment condition, e.g., in the presence of NOM and other aqueous constituents. OP pesticides, in the phosphorothioate subgroup, have been found to be transformed to their corresponding oxon in the presence of free chlorine, and phosphate esters have been found to undergo chlorine assisted hydrolysis. However, only rate coefficients for the oxidation of diazinon have been reported.<sup>18</sup> Therefore, the need exists to systematically investigate chlorination of OP pesticides as a class and determine if reactivity with aqueous chlorine is related in a predictable way to OP chemical structure. If a relationship between reactivity and pesticide structure exists, the ability to predict the fate of OP pesticides in the presence of free chlorine would greatly aid regulators in assuring that tolerances to OP pesticide exposure are not exceeded. After developing predictive tools for the entire class of OP pesticides, we plan to address other important classes of pesticides and toxic chemicals.

## 5 REFERENCES

- (1) Kolpin, D. W.; Furlong, E. T.; Meyer, M. T.; Thurman, E. M.; Zaugg, S. D.; Barber, L. B.; Buxton, H. T. *Environmental Science & Technology* **2002**, *36*, 1202-1211.
- (2) Squillace, P. J.; Scott, J. C.; Moran, M. J.; Nolan, B. T.; Kolpin, D. W. *Environmental Science & Technology* **2002**, *36*, 1923-1930.
- (3) Miltner, R. J.; Baker, D. B.; Speth, T. F.; Fronk, C. A. *Journal American Water Works Association* **1989**, *81*, 43-52.
- (4) Pinkston, K. E.; Sedlak, D. L. *Environmental Science & Technology* **2004**, *38*, 4019-4025.
- (5) Dodd, M. C.; Huang, C. H. *Environmental Science & Technology* **2004**, *38*, 5607-5615.
- (6) Deborde, M.; Rabouan, S.; Gallard, H.; Legube, B. *Environmental Science & Technology* **2004**, *38*, 5577-5583.
- (7) Hu, J. Y.; Cheng, S. J.; Aizawa, T.; Terao, Y.; Kunikane, S. *Environmental Science & Technology* **2003**, *37*, 5665-5670.
- (8) Kolpin, D. W.; Barbash, J. E.; Gilliom, R. J. *Ground Water* **2000**, *38*, 858-863.
- (9) Verstraeten, I. M.; Thurman, E. M.; Lindsey, M. E.; Lee, E. C.; Smith, R. D. *Journal of Hydrology* **2003**, *276*, 287-288.
- (10) Coupe, R. H.; Blomquist, J. D. *Journal American Water Works Association* **2004**, *96*, 56-68.
- (11) *Community Water System Survey*; United States Environmental Protection Agency, 1997; Vol. 1, EPA 815-R-97-011a.
- (12) Lopez, A.; Mascolo, G.; Tiravanti, G.; Santori, M.; Passino, R. *Water Science and Technology* **1994**, *30*, 53-59.
- (13) Mascolo, G.; Lopez, A.; Passino, R.; Ricco, G.; Tiravanti, G. *Water Research* **1994**, *28*, 2499-2506.
- (14) Adams, C. D.; Randtke, S. J. *Journal American Water Works Association* **1992**, *84*, 91-102.
- (15) Miles, C. J. *Environmental Science & Technology* **1991**, *25*, 1774-1779.
- (16) Mason, Y. Z.; Choshen, E.; Ravacha, C. *Water Research* **1990**, *24*, 11-21.
- (17) Kodama, S.; Yamamoto, A.; Matsunaga, A. *Journal of Agricultural and Food Chemistry* **1997**, *45*, 990-994.
- (18) Zhang, Q.; Pehkonen, S. O. *Journal of Agricultural and Food Chemistry* **1999**, *47*, 1760-1766.
- (19) Magara, Y.; Aizawa, T.; Matumoto, N.; Souna, F. *Water Science and Technology* **1994**, *30*, 119-128.
- (20) Wu, J. G.; Laird, D. A. *Environmental Toxicology and Chemistry* **2003**, *22*, 261-264.
- (21) Wolfe, N. L. *Chemosphere* **1980**, *9*, 571-579.
- (22) *Standard Methods for the Examination of Water and Wastewater*; 20 ed.; APHA, AWWA, and WEF: Washington D.C., 1998.
- (23) Liu, B.; McConnell, L. L.; Torrents, A. *Chemosphere* **2001**, *44*, 1315-1323.
- (24) Snoeyink, V. L.; Jenkins, D. A. *Water Chemistry*; John Wiley & Sons: New York, NY, 1980.

- (25) Macalady, D. L.; Wolfe, N. L. *Journal of Agricultural and Food Chemistry* **1983**, *31*, 1139-1147.
- (26) Reckhow, D. A.; Platt, T. L.; MacNeill, A. L.; McClellan, J. N. *Journal of Water Supply Research and Technology-Aqua* **2001**, *50*, 1-13.
- (27) Rebenne, L. M.; Gonzalez, A. C.; Olson, T. M. *Environmental Science & Technology* **1996**, *30*, 2235-2242.
- (28) Arotzky, J.; Symons, M. C. R. *Quarterly Reviews* **1962**, *16*, 282-297.
- (29) Wang, T. X.; Margerum, D. W. *Inorganic Chemistry* **1994**, *33*, 1050-1055.



**TABLES**

Table 1 Stoichiometric equations and rate coefficients used in the chlorpyrifos degradation pathway model. Numbers in parenthesis are 95% confidence intervals for the rate coefficients determined in this study.

	Reaction Stoichiometry	Rate/Equilibrium Coefficient (25 °C)	Reference
1	$\text{HOCl} + \text{CP} \xrightarrow{k_r} \text{CPO} + \text{H}^+ + \text{Cl}^- + \text{S}$	$k_r = 1.72 (\pm 0.68) \times 10^6 \text{ M}^{-1} \text{ h}^{-1}$	This work
2	$\text{CP} \xrightarrow{k_{h,\text{CP}}} \text{TCP}$	$k_{h,\text{CP}} = k_{N,\text{CP}} + k_{B,\text{CP}}[\text{OH}^-]$ $k_{N,\text{CP}} = 3.72 \times 10^{-4} \text{ h}^{-1}$ $k_{B,\text{CP}} = 37.0 \text{ M}^{-1} \text{ h}^{-1}$	25
3	$\text{CPO} \xrightarrow{k_{h,\text{CPO}}} \text{TCP}$	$k_{h,\text{CPO}} = k_{N,\text{CPO}} + k_{B,\text{CPO}}[\text{OH}^-]$ $k_{N,\text{CPO}} = 2.13 (\pm 1.73) \times 10^{-3} \text{ h}^{-1}$ $k_{B,\text{CPO}} = 230 (\pm 19) \text{ M}^{-1} \text{ h}^{-1}$	This work
4	$\text{CP} + \text{OCl}^- \xrightarrow{k_{\text{OCl},\text{CP}}} \text{TCP} + \text{Cl}^-$	$k_{\text{OCl},\text{CP}} = 990 (\pm 200) \text{ M}^{-1} \text{ h}^{-1}$	This work
5	$\text{CPO} + \text{OCl}^- \xrightarrow{k_{\text{OCl},\text{CPO}}} \text{TCP} + \text{Cl}^-$	$k_{\text{OCl},\text{CPO}} = 1340 (\pm 110) \text{ M}^{-1} \text{ h}^{-1}$	This work
6	$\text{HOCl} \longleftrightarrow \text{OCl}^- + \text{H}^+$	$\text{pK}_a = 7.5$	24

**FIGURES**

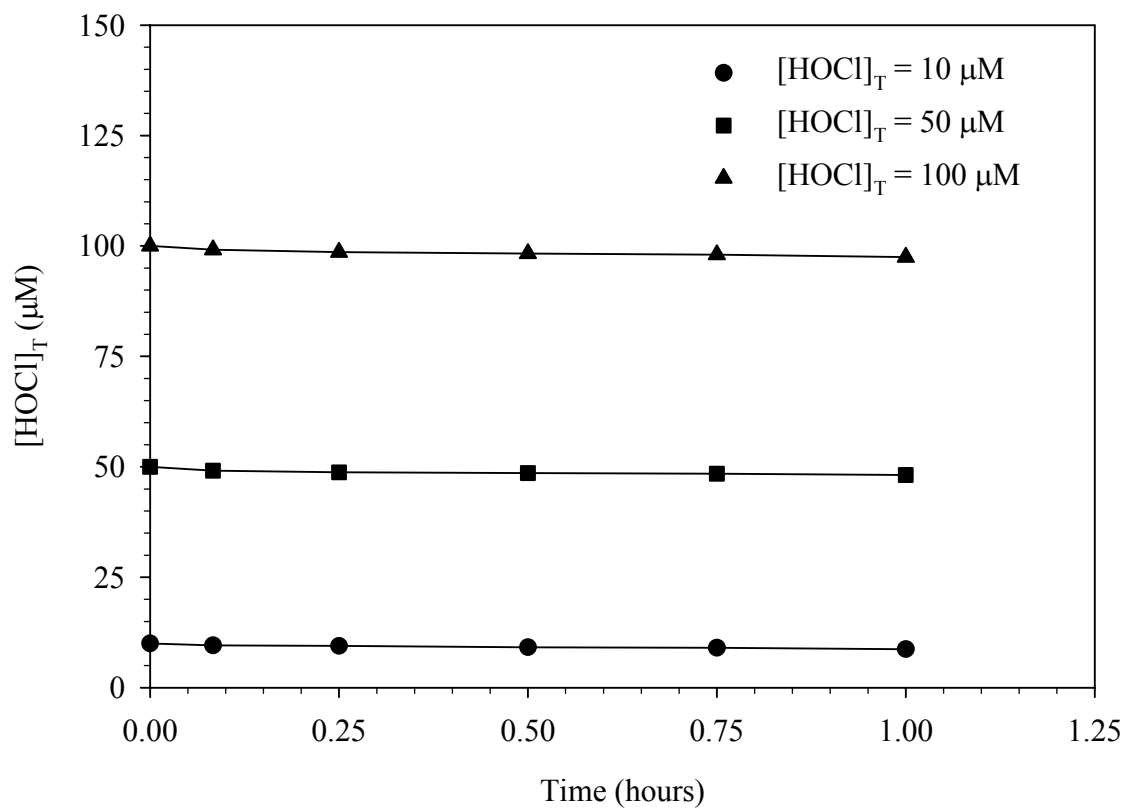


Figure 1 Free chlorine loss in the presence of CP at pH 8.5.  $[\text{CP}]_0 = 0.5 \mu\text{M}$ ,  $[\text{CO}_3]_T = 10 \text{ mM}$ , Temperature =  $25 \text{ }^\circ\text{C}$ , and  $[\text{HOCl}]_T = 10, 50, 100 \mu\text{M}$ .

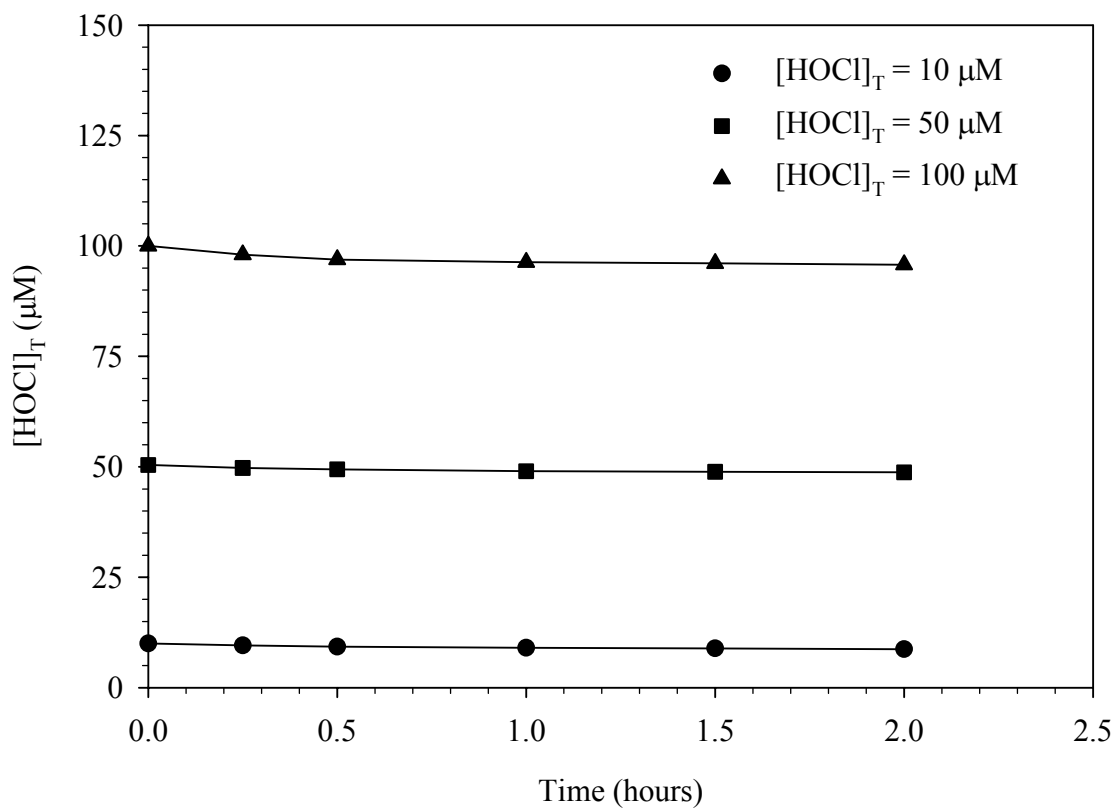


Figure 2 Free chlorine loss in the presence of CP at pH 9.  $[\text{CP}]_o = 0.5 \mu\text{M}$ ,  $[\text{CO}_3]_T = 10 \text{ mM}$ , Temperature =  $25 \text{ }^\circ\text{C}$ , and  $[\text{HOCl}]_T = 10, 50, 100 \mu\text{M}$ .

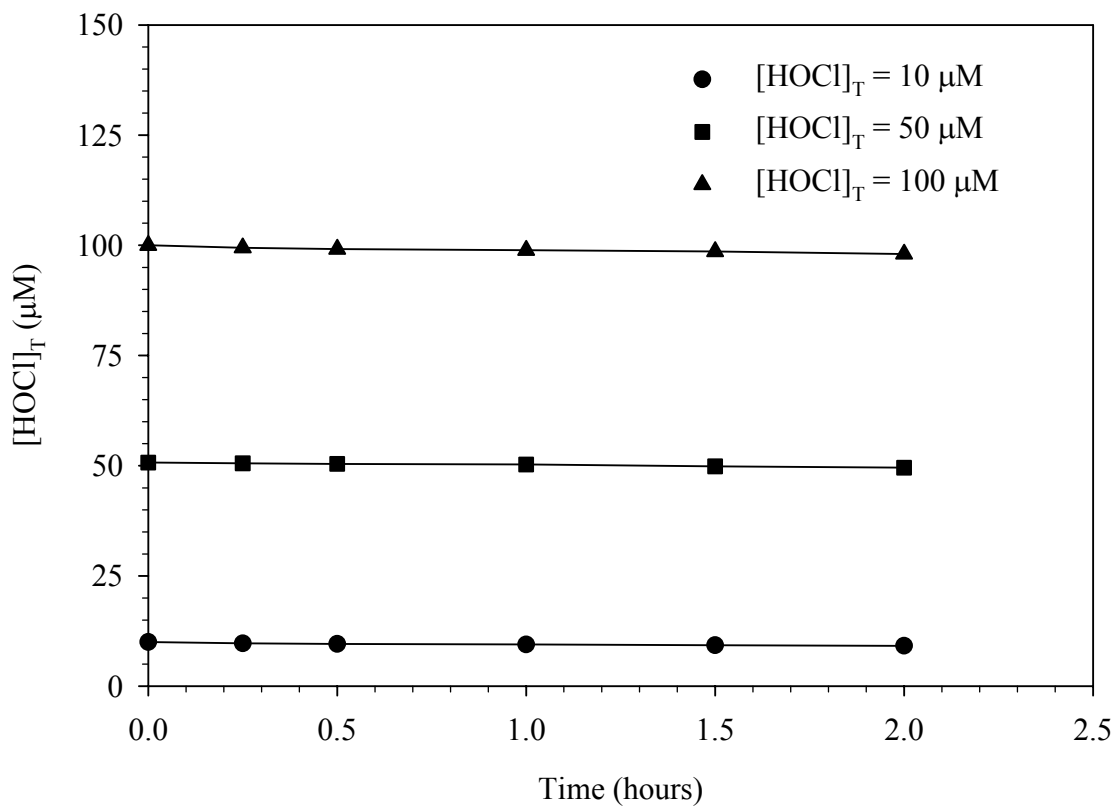


Figure 3 Free chlorine loss in the presence of CP at pH 10.  $[\text{CP}]_0 = 0.5 \mu\text{M}$ ,  $[\text{CO}_3]_T = 10 \text{ mM}$ , Temperature = 25 °C, and  $[\text{HOCl}]_T = 10, 50, 100 \mu\text{M}$ .

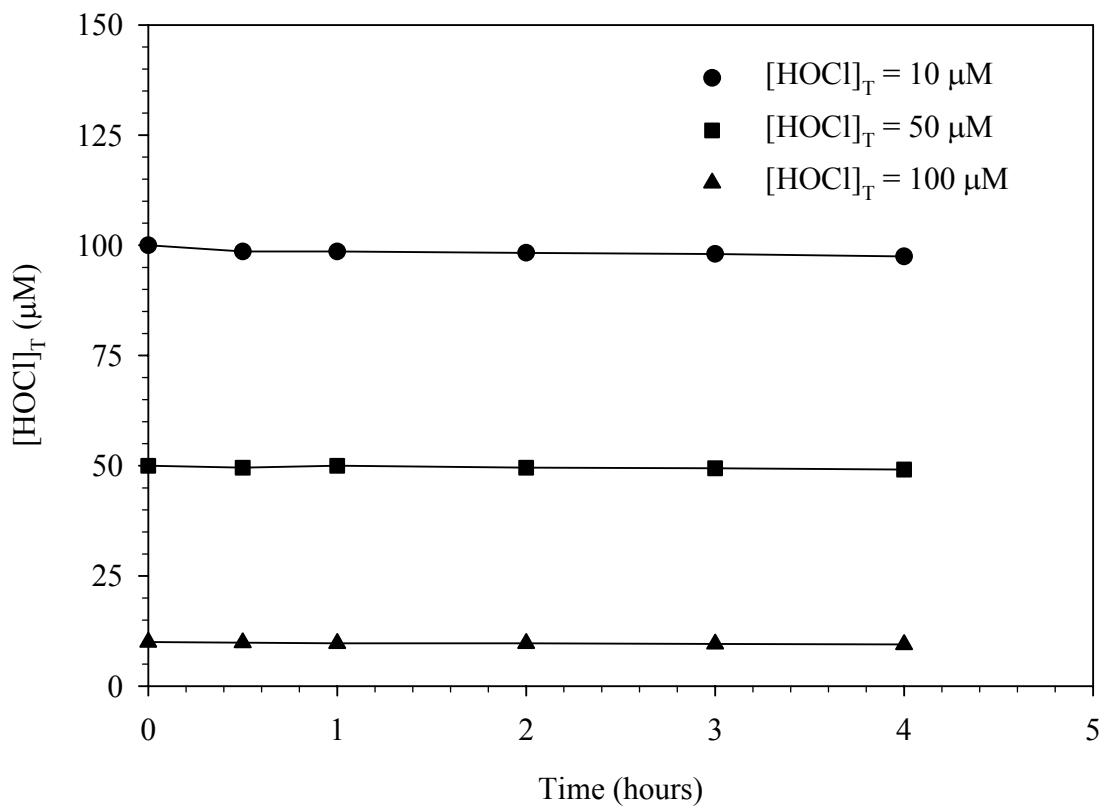


Figure 4 Free chlorine loss in the presence of CP at pH 11.  $[\text{CP}]_0 = 0.5 \mu\text{M}$ ,  $[\text{CO}_3]_T = 10 \text{ mM}$ , Temperature =  $25 \text{ }^\circ\text{C}$ , and  $[\text{HOCl}]_T = 10, 50, 100 \mu\text{M}$ .

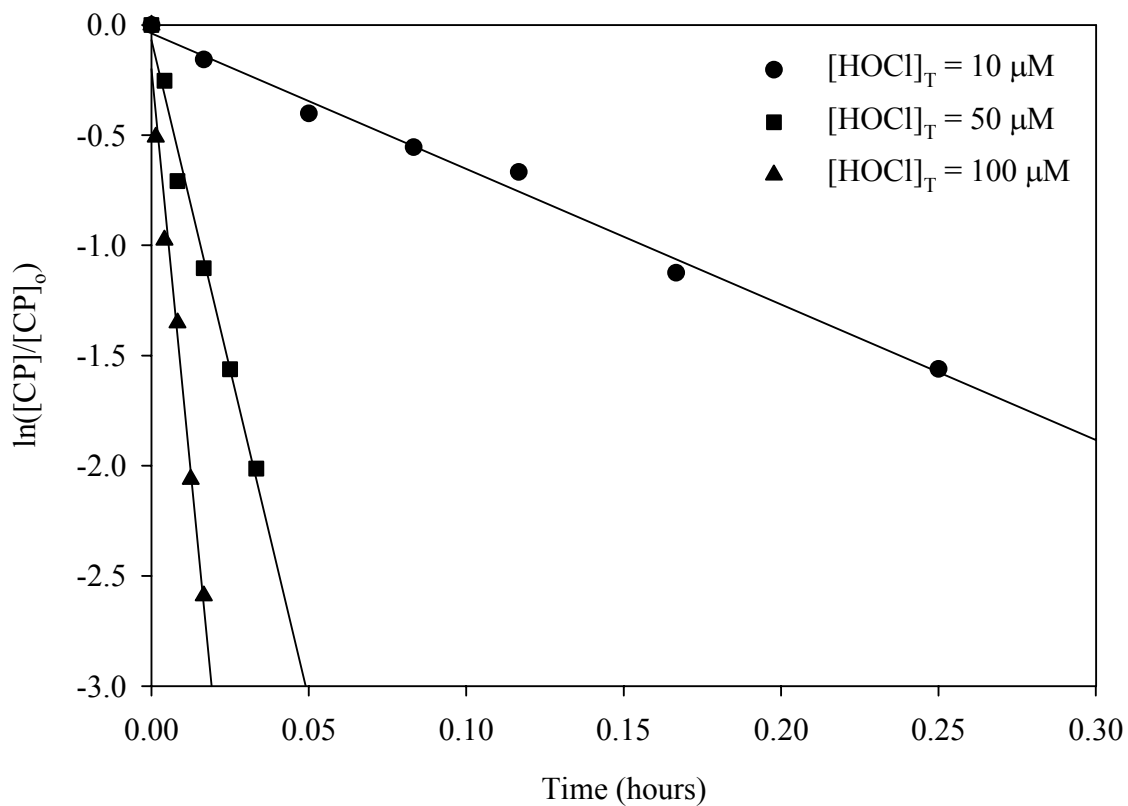


Figure 5 Observed first order loss of CP as a function of free chlorine at pH 6.36.  $[CP]_0 = 0.5 \mu M$ ,  $[PO_4]_T = 10 \text{ mM}$ , Temperature =  $25 \text{ }^\circ\text{C}$ , and  $[HOCl]_T = 10, 50, 100 \mu M$ .



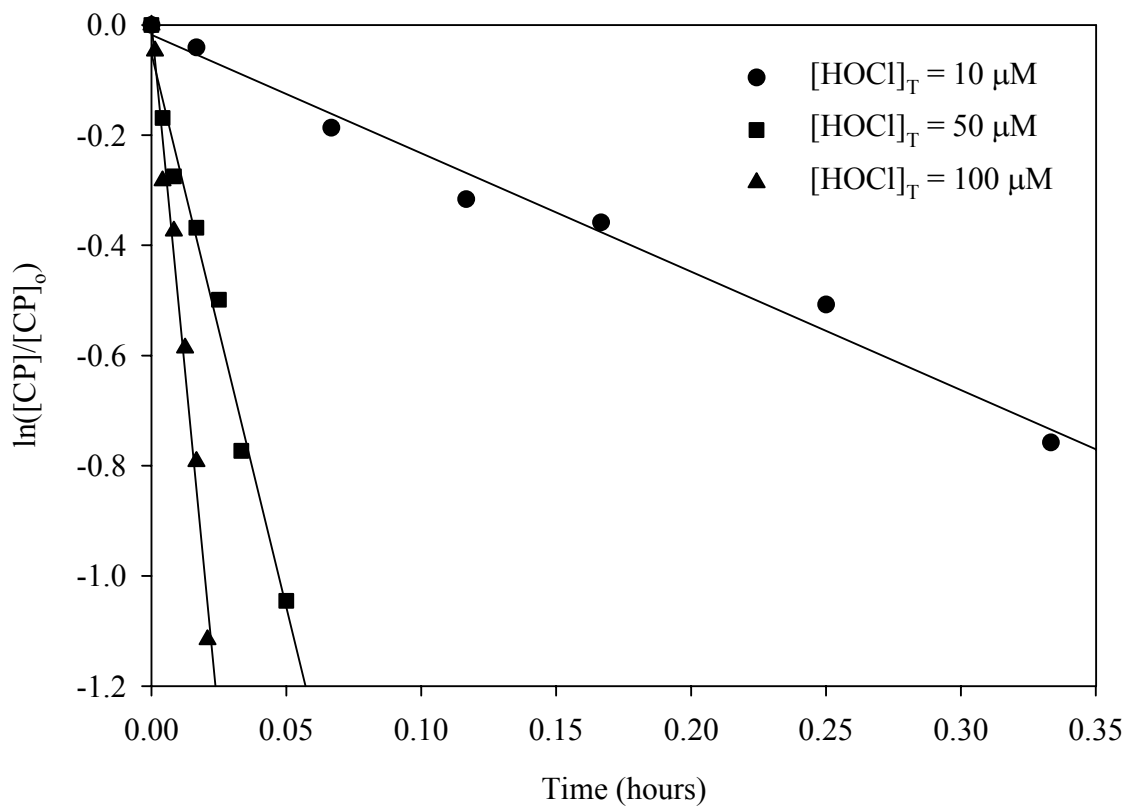


Figure 6 Observed first order loss of CP as a function of free chlorine at pH 7.5.  $[CP]_0 = 0.5 \mu M$ ,  $[PO_4]_T = 10 \text{ mM}$ , Temperature = 25 °C, and  $[HOCl]_T = 10, 50, 100 \mu M$ .

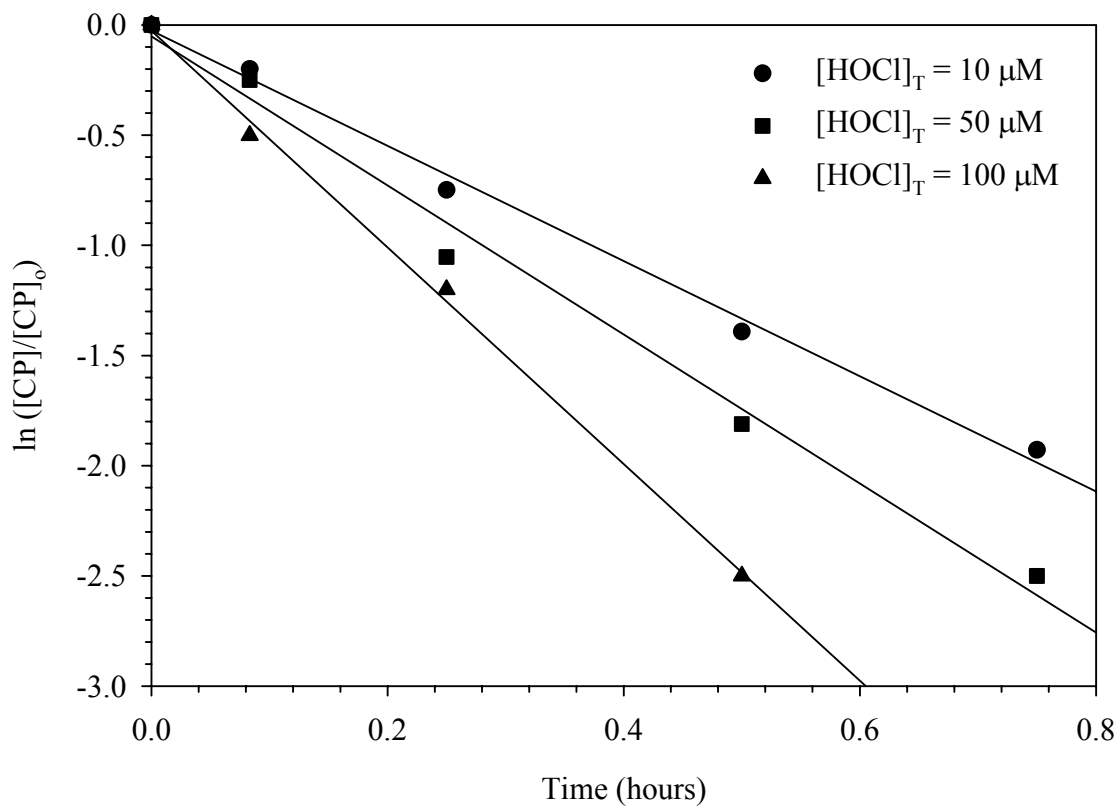


Figure 7 Observed first order loss of CP as a function of free chlorine at pH 8.5.  $[CP]_0 = 0.5 \mu M$ ,  $[CO_3]_T = 10 \text{ mM}$ , Temperature =  $25 \text{ }^\circ\text{C}$ , and  $[HOCl]_T = 10, 50, 100 \mu M$ .

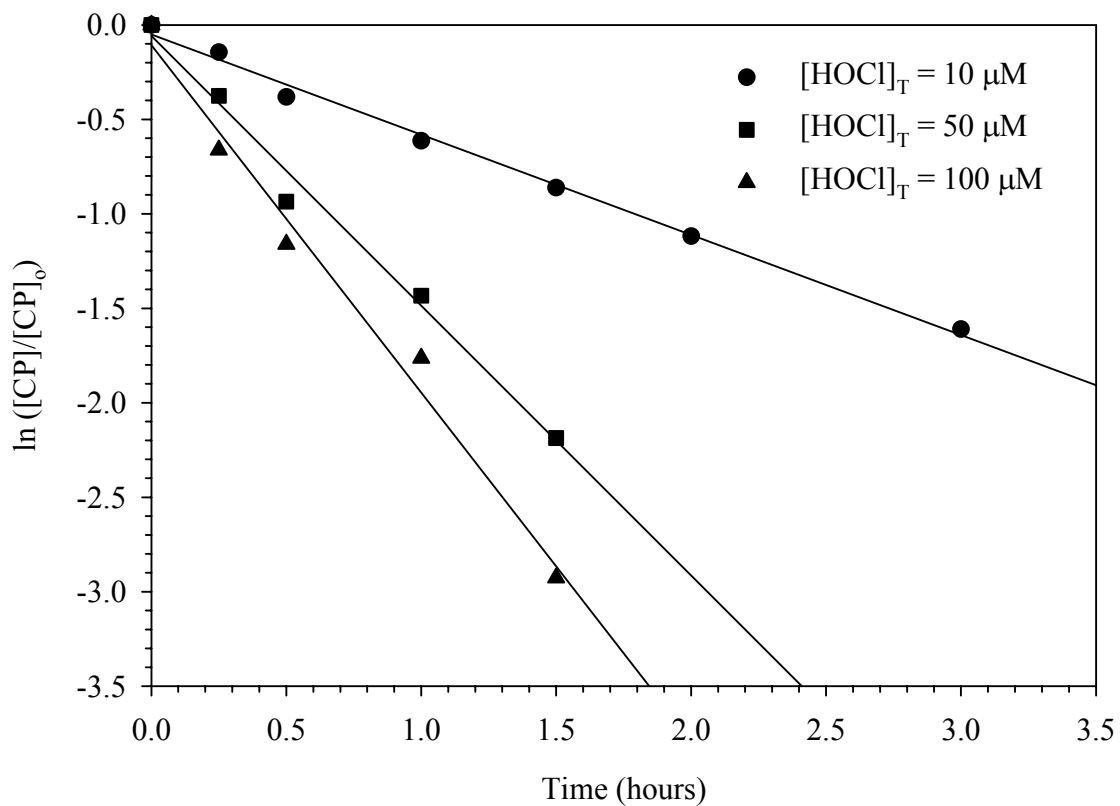


Figure 8 Observed first order loss of CP as a function of free chlorine at pH 8.75.  $[CP]_0 = 0.5 \mu M$ ,  $[CO_3]_T = 10 \text{ mM}$ , Temperature =  $25 \text{ }^\circ\text{C}$ , and  $[HOCl]_T = 10, 50, 100 \mu M$ .

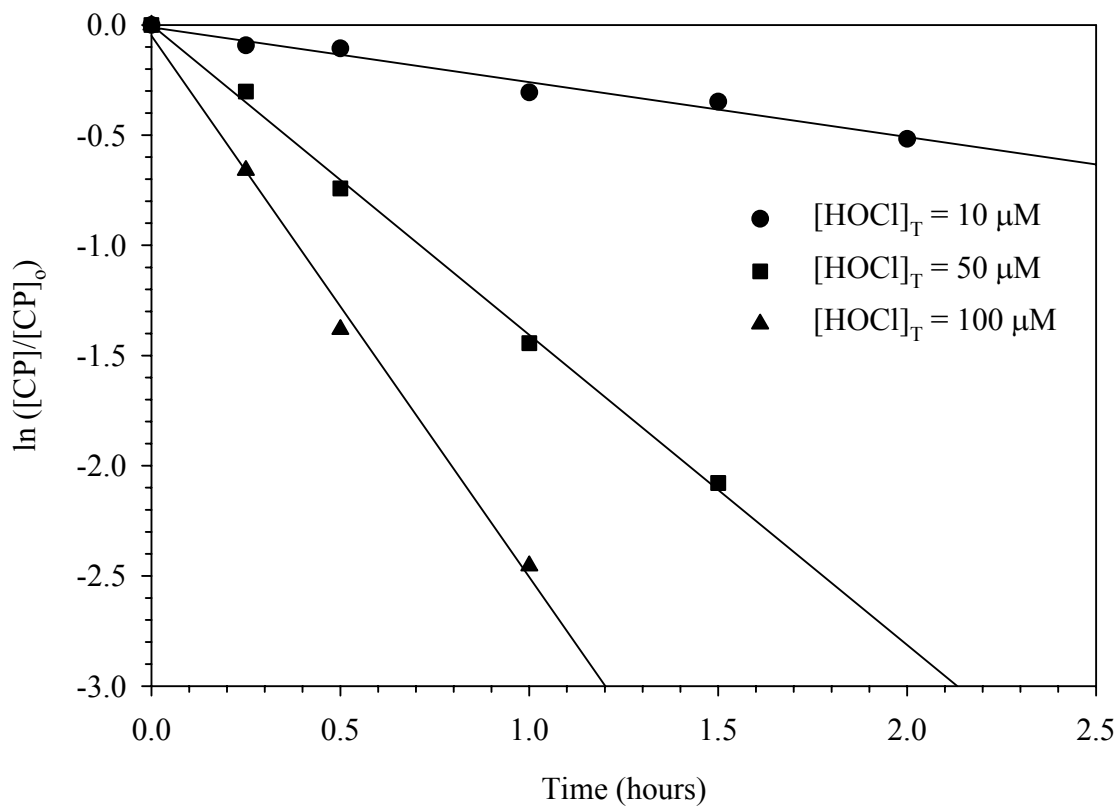


Figure 9 Observed first order loss of CP as a function of free chlorine at pH 9.  $[CP]_0 = 0.5 \mu M$ ,  $[CO_3]_T = 10 \text{ mM}$ , Temperature =  $25 \text{ }^\circ\text{C}$ , and  $[HOCl]_T = 10, 50, 100 \mu M$ .

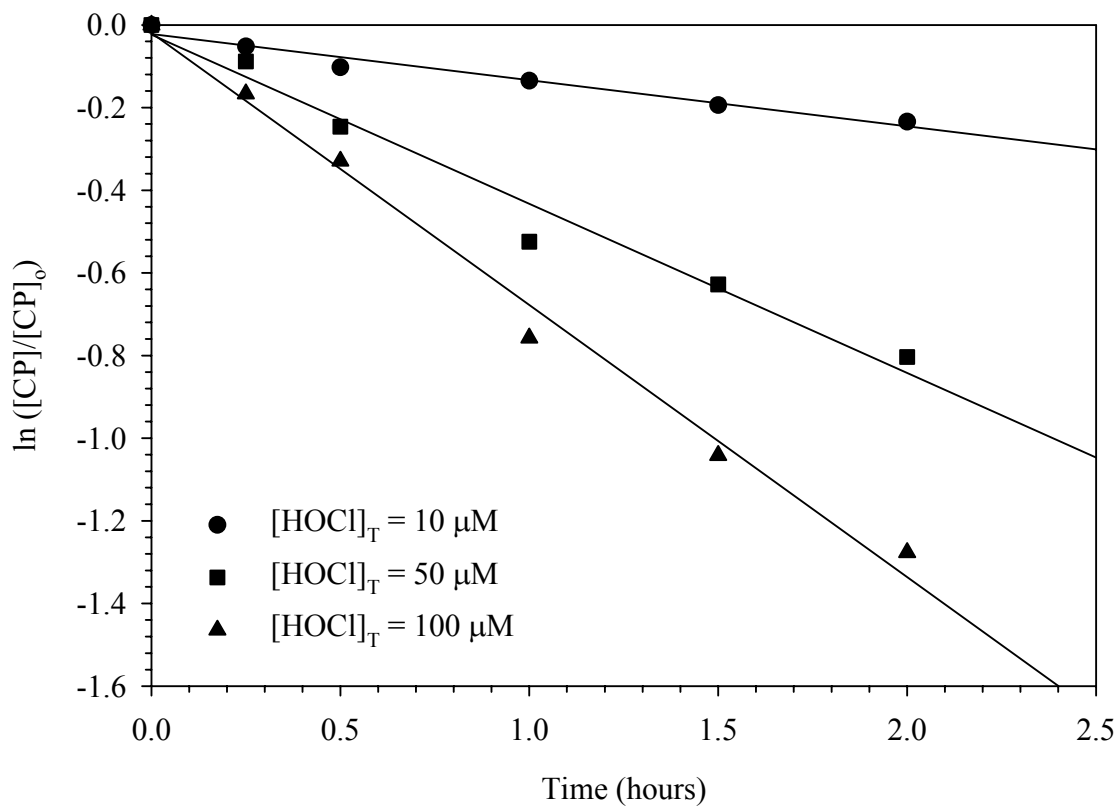


Figure 10 Observed first order loss of CP as a function of free chlorine at pH 10.  $[CP]_0 = 0.5 \mu M$ ,  $[CO_3]_T = 10 \text{ mM}$ , Temperature =  $25 \text{ }^\circ\text{C}$ , and  $[HOCl]_T = 10, 50, 100 \mu M$ .

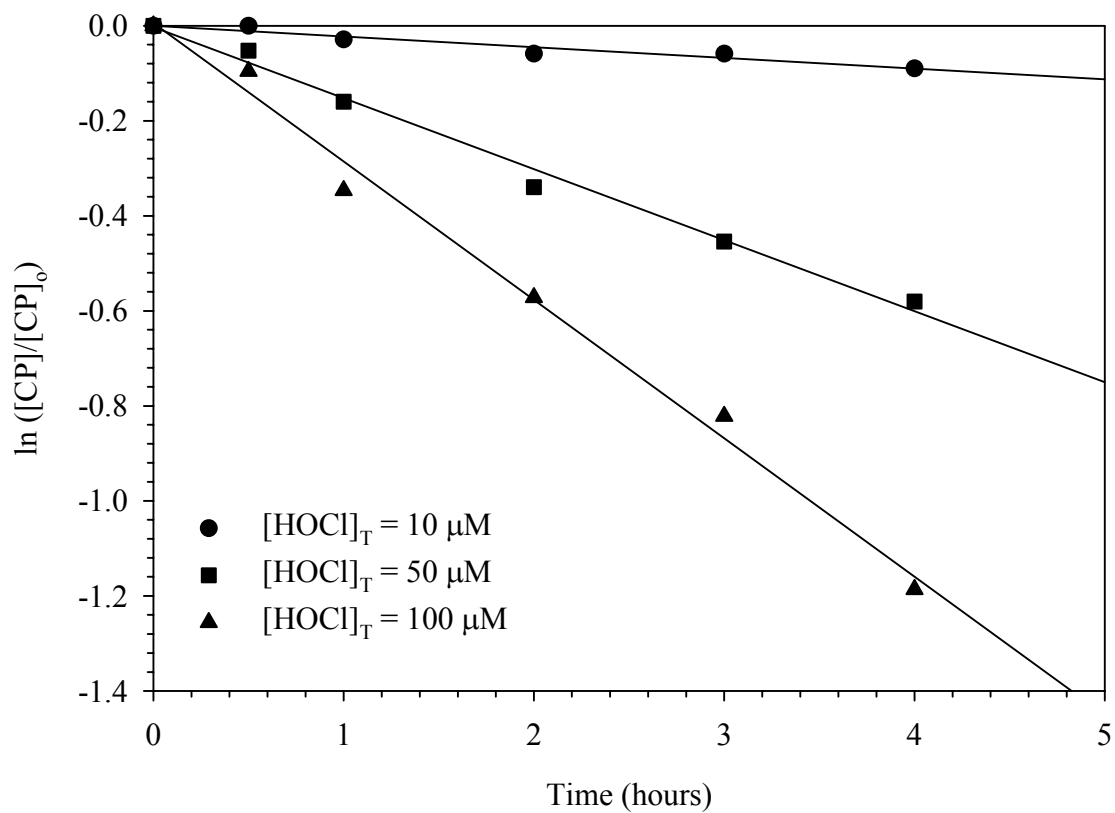


Figure 11 Observed first order loss of CP as a function of free chlorine at pH 11.  $[CP]_0 = 0.5 \mu M$ ,  $[CO_3]_T = 10 \text{ mM}$ , Temperature =  $25 \text{ }^\circ\text{C}$ , and  $[HOCl]_T = 10, 50, 100 \mu M$ .

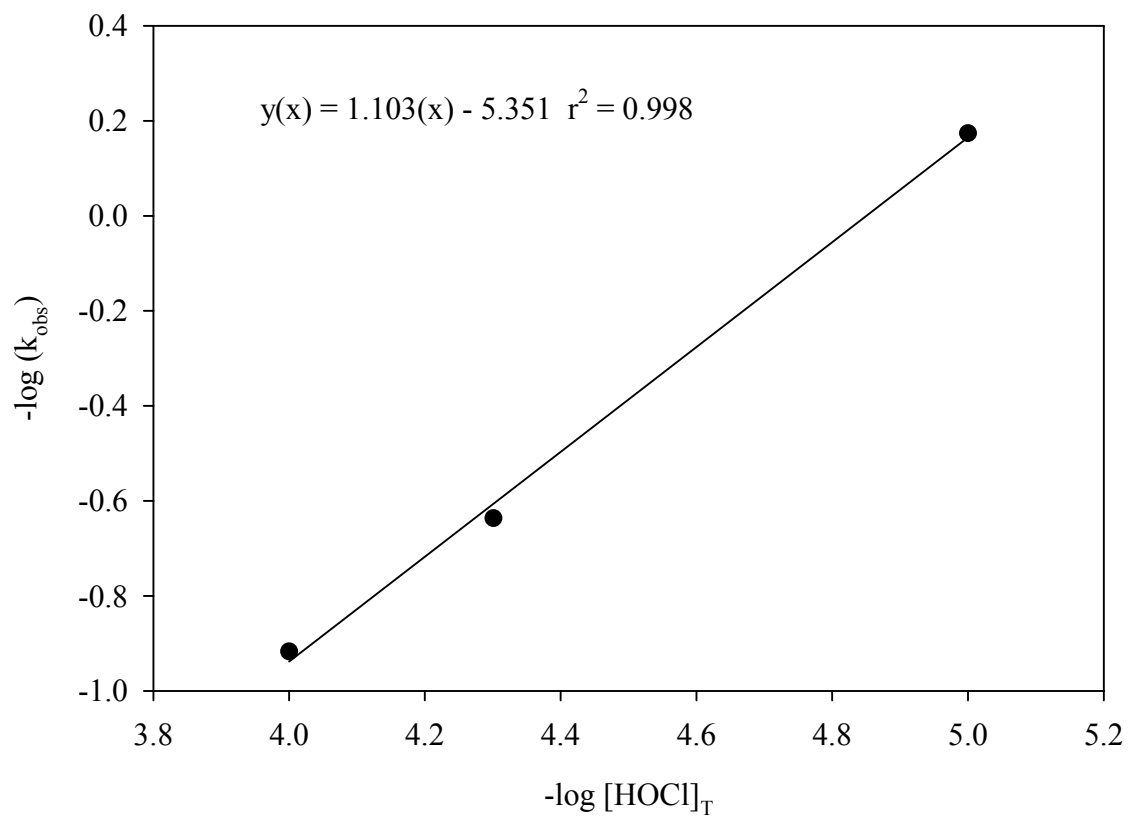


Figure 12 Reaction order of free chlorine with CP at pH 8.5.  $[\text{CP}]_0 = 0.5 \mu\text{M}$ ,  $[\text{CO}_3]_T = 10 \text{ mM}$ , Temperature = 25 °C, and  $[\text{HOCl}]_T = 10, 50, 100 \mu\text{M}$ .

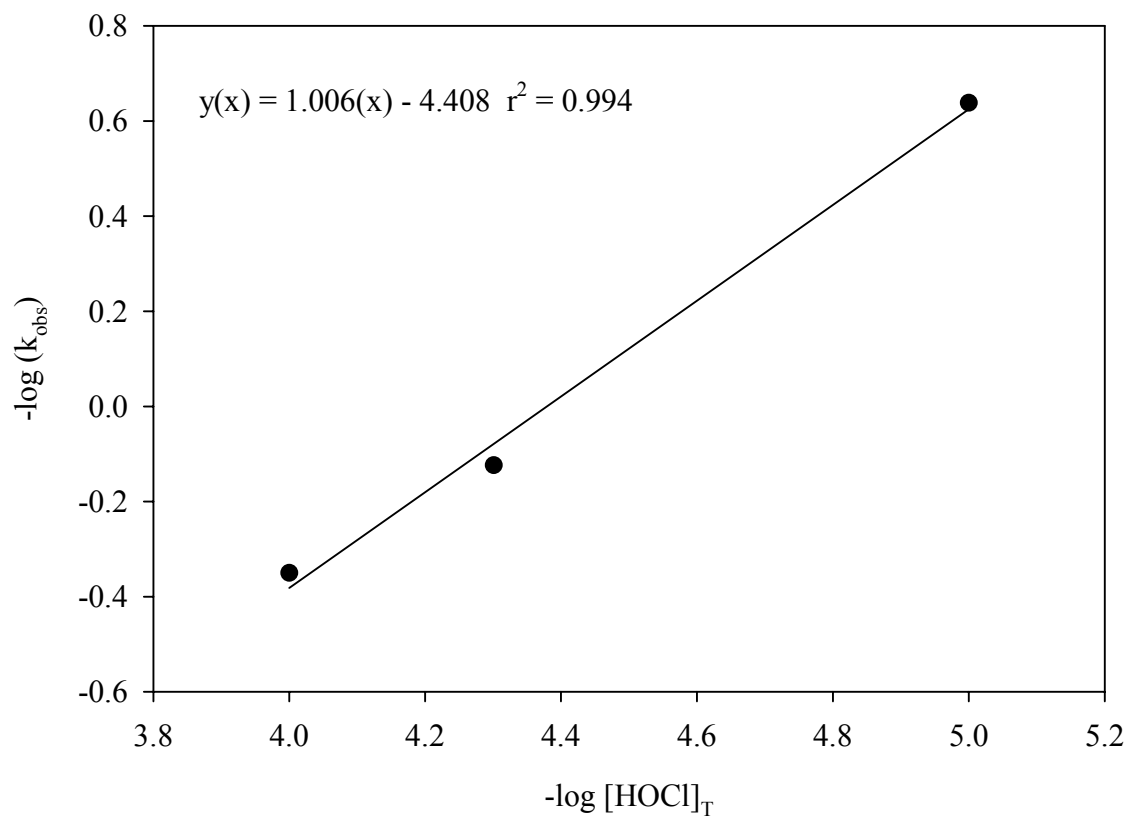


Figure 13 Reaction order of free chlorine with CP at pH 9.0.  $[\text{CP}]_0 = 0.5 \mu\text{M}$ ,  $[\text{CO}_3]_T = 10 \text{ mM}$ , Temperature = 25 °C, and  $[\text{HOCl}]_T = 10, 50, 100 \mu\text{M}$ .



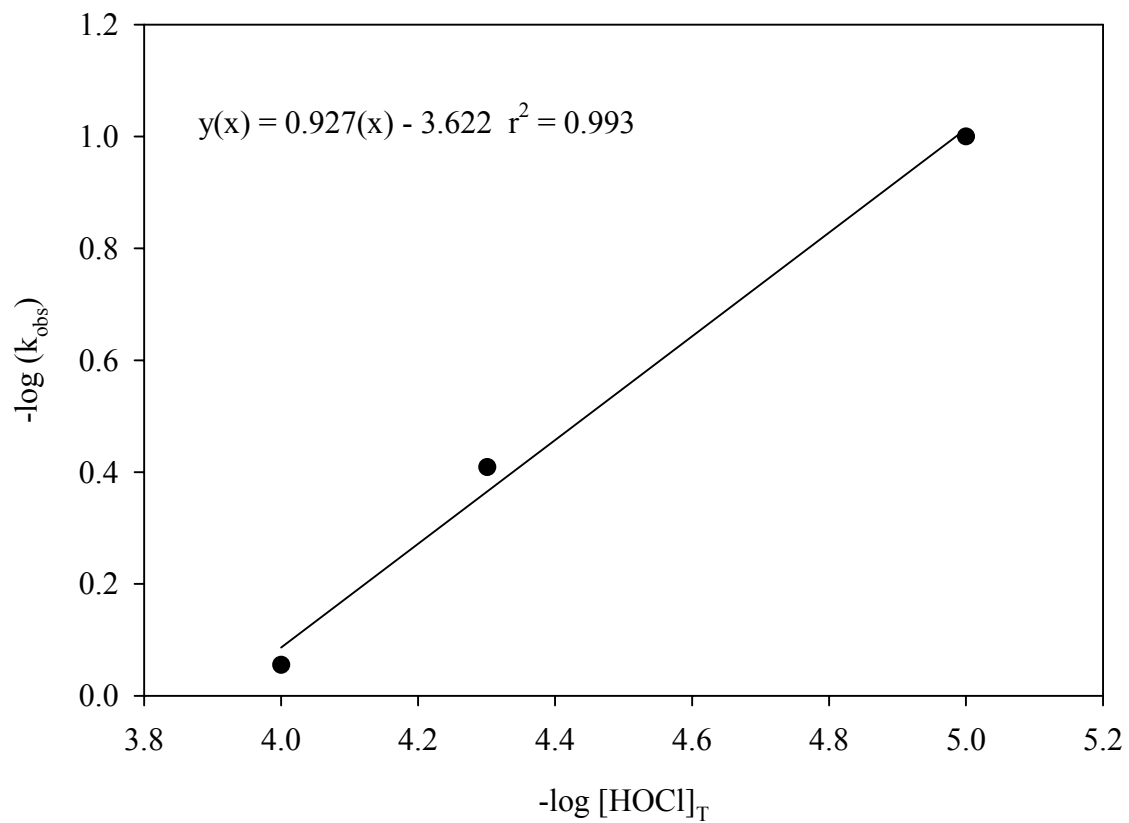


Figure 14 Reaction order of free chlorine with CP at pH 10.  $[\text{CP}]_0 = 0.5 \mu\text{M}$ ,  $[\text{CO}_3]_T = 10 \text{ mM}$ , Temperature =  $25^\circ\text{C}$ , and  $[\text{HOCl}]_T = 10, 50, 100 \mu\text{M}$ .

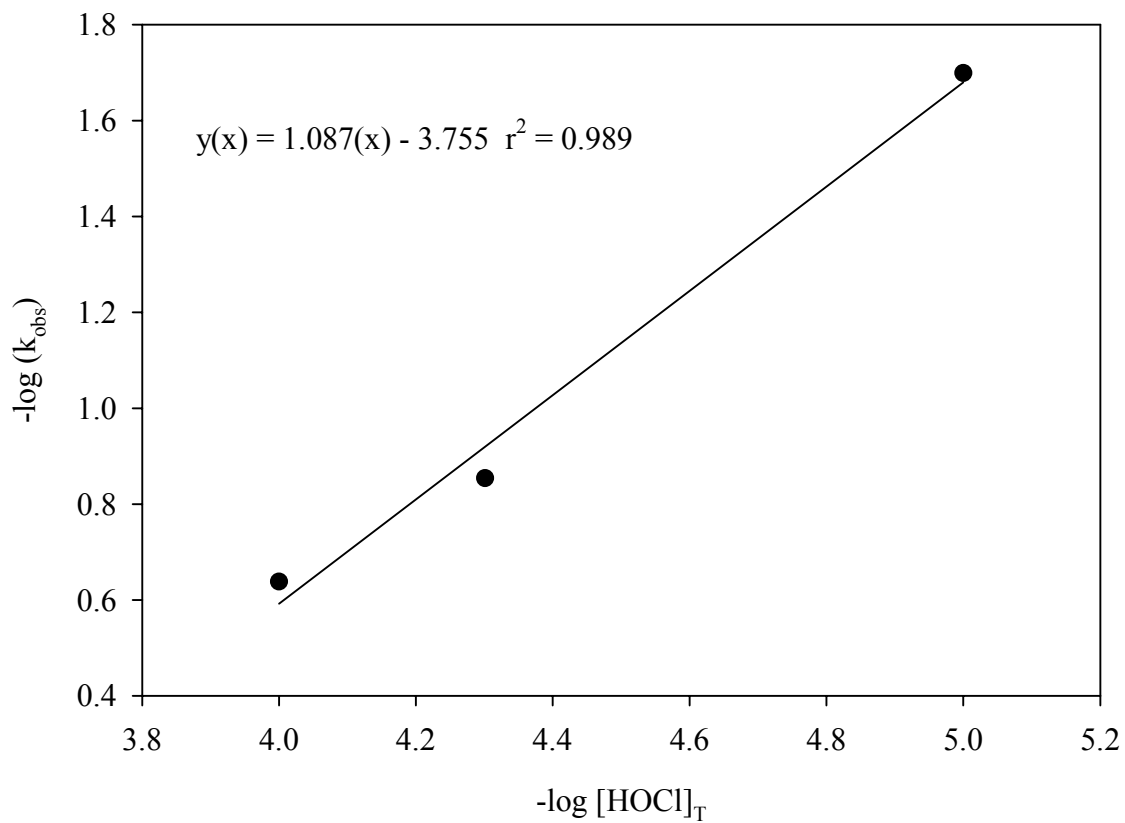


Figure 15 Reaction order of free chlorine with CP at pH 11.  $[\text{CP}]_0 = 0.5 \mu\text{M}$ ,  $[\text{CO}_3]_T = 10 \text{ mM}$ , Temperature =  $25^\circ\text{C}$ , and  $[\text{HOCl}]_T = 10, 50, 100 \mu\text{M}$ .

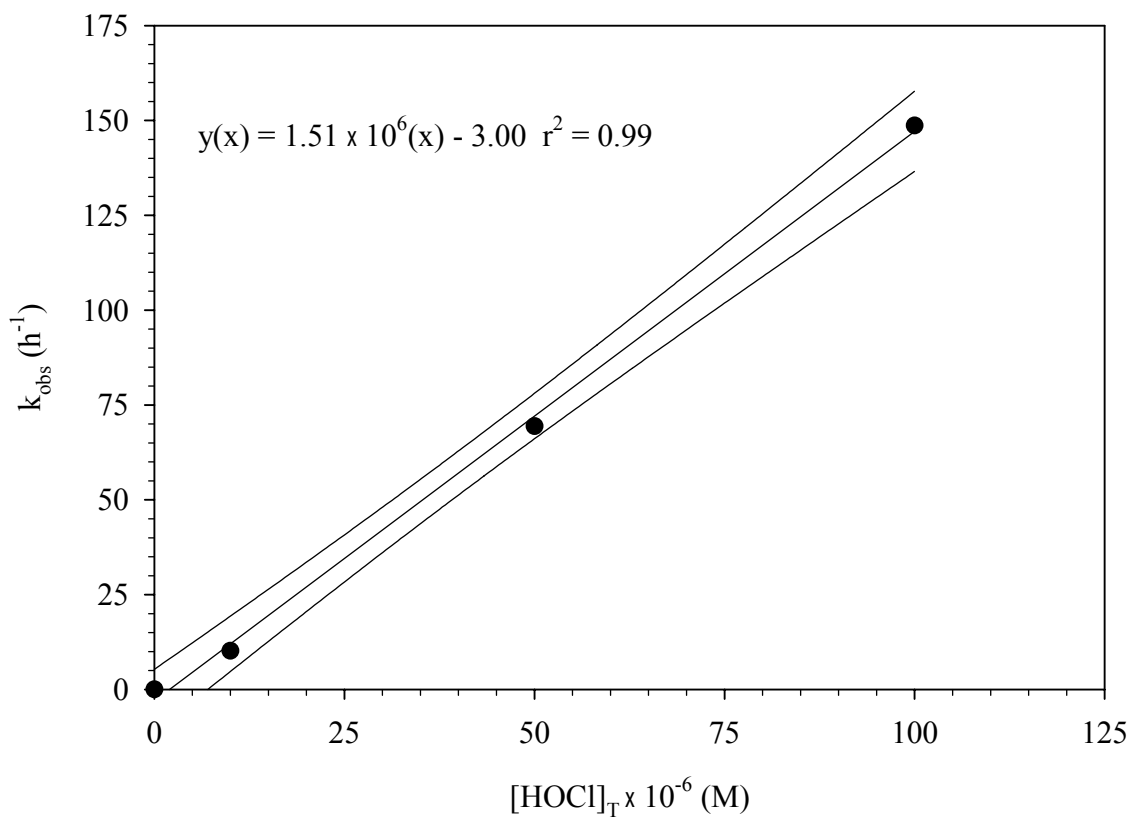


Figure 16 Apparent second order reaction rate coefficient for CP in the presence of free chlorine at pH 6.36.  $[\text{CP}]_0 = 0.5 \mu\text{M}$ ,  $[\text{PO}_4]_{\text{T}} = 10 \text{ mM}$ , Temperature =  $25 \text{ }^\circ\text{C}$ , and  $[\text{HOCl}]_{\text{T}} = 10, 50, 100 \mu\text{M}$ . 95% confidence intervals about the regression line shown.

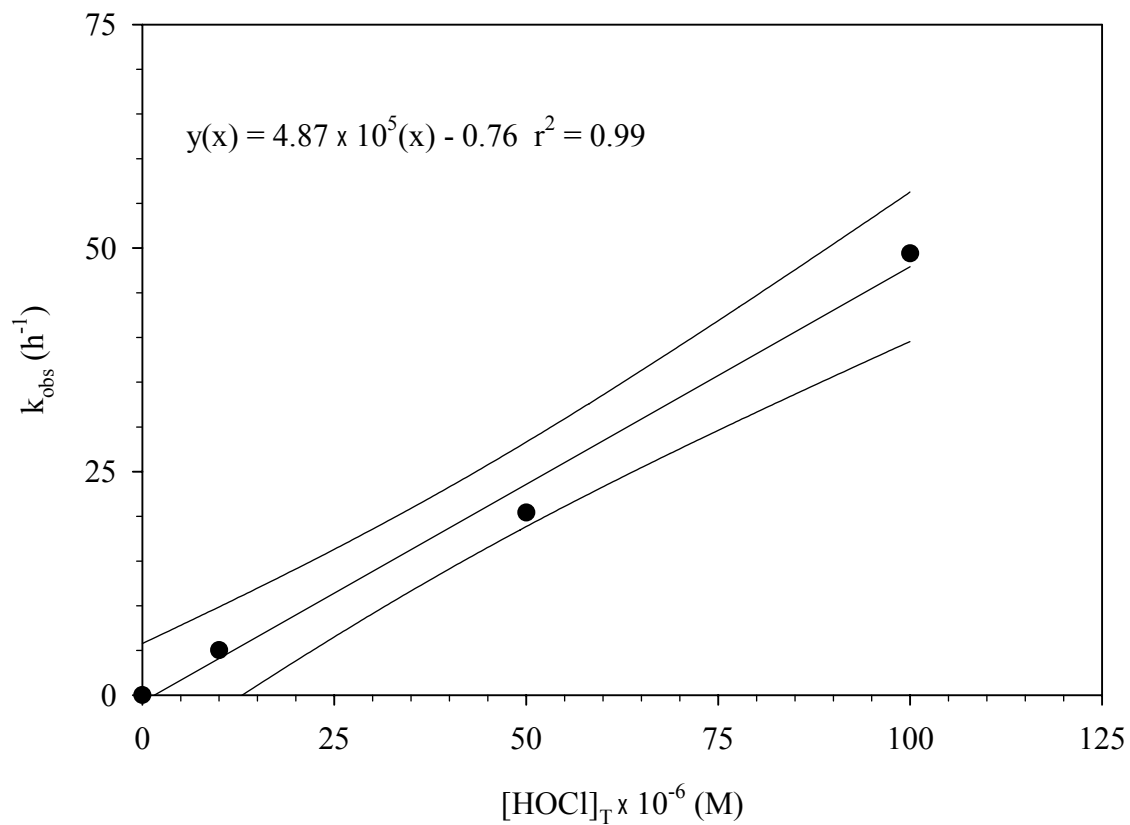


Figure 17 Apparent second order reaction rate coefficient for CP in the presence of free chlorine at pH 7.5.  $[\text{CP}]_0 = 0.5 \mu\text{M}$ ,  $[\text{PO}_4]_{\text{T}} = 10 \text{ mM}$ , Temperature = 25 °C, and  $[\text{HOCl}]_{\text{T}} = 10, 50, 100 \mu\text{M}$ . 95% confidence intervals about the regression line shown.

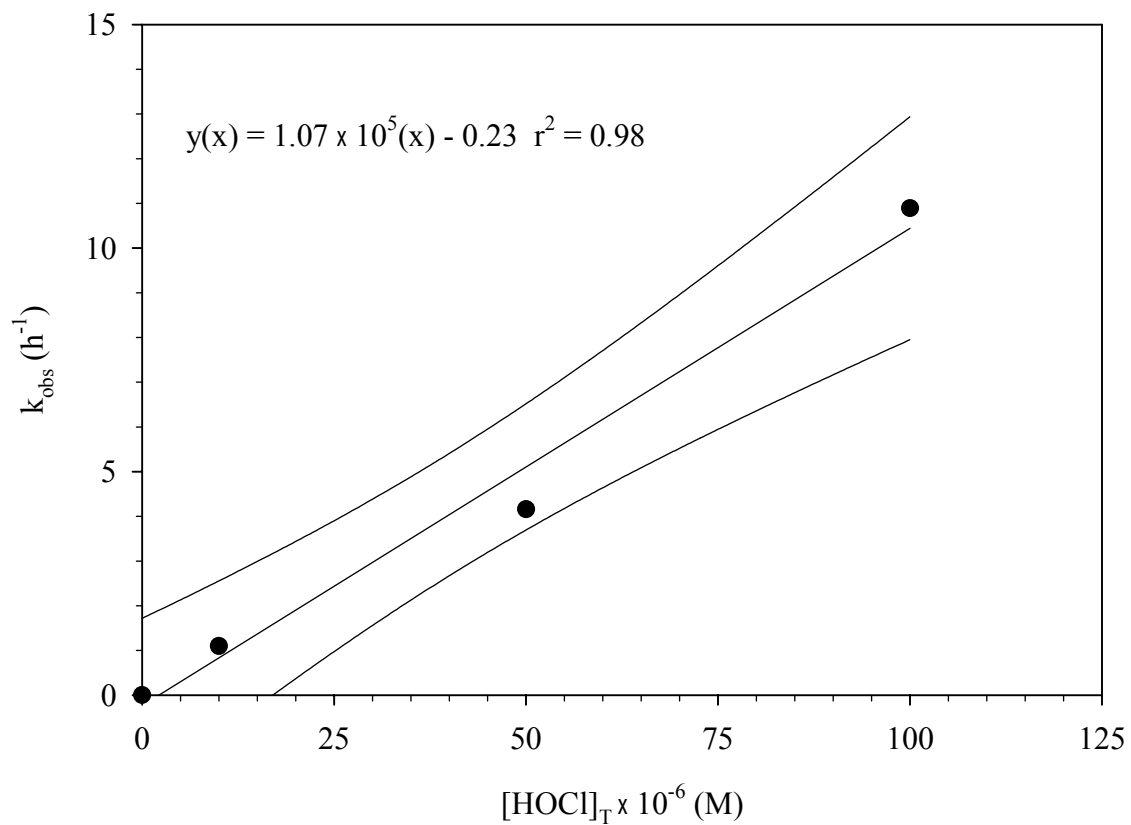


Figure 18 Apparent second order reaction rate coefficient for CP in the presence of free chlorine at pH 8.5.  $[\text{CP}]_0 = 0.5 \mu\text{M}$ ,  $[\text{PO}_4]_T = 10 \text{ mM}$ , Temperature = 25 °C, and  $[\text{HOCl}]_T = 10, 50, 100 \mu\text{M}$ . 95% confidence intervals about the regression line shown.

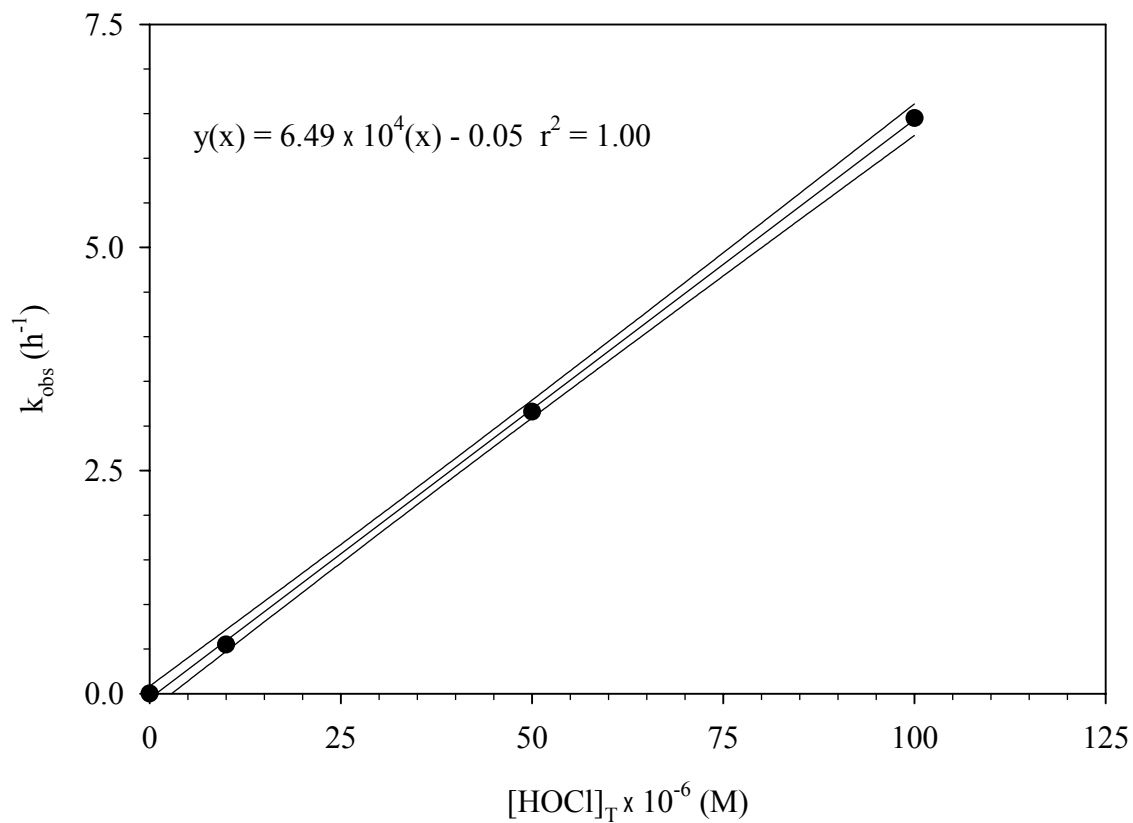


Figure 19 Apparent second order reaction rate coefficient for CP in the presence of free chlorine at pH 8.75.  $[CP]_0 = 0.5 \mu\text{M}$ ,  $[\text{CO}_3]_T = 10 \text{ mM}$ , Temperature =  $25 \text{ }^\circ\text{C}$ , and  $[\text{HOCl}]_T = 10, 50, 100 \mu\text{M}$ . 95% confidence intervals about the regression line shown.

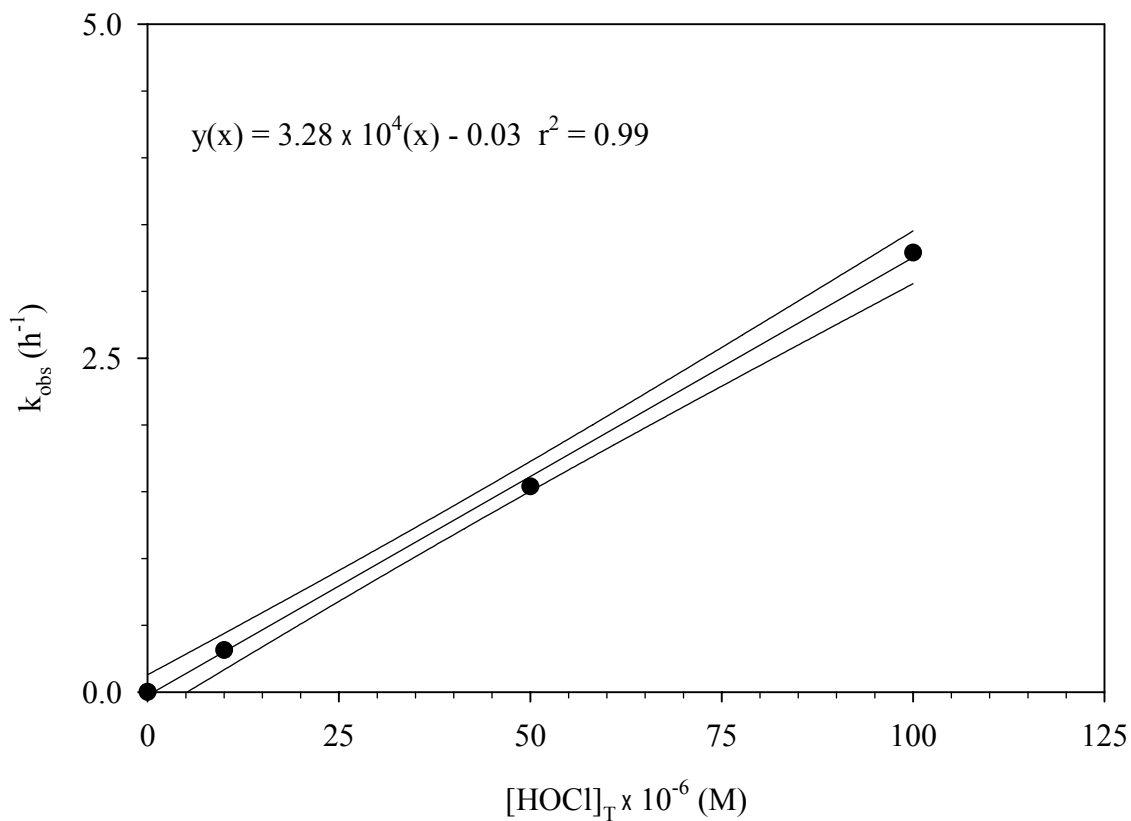


Figure 20 Apparent second order reaction rate coefficient for CP in the presence of free chlorine at pH 9.  $[\text{CP}]_0 = 0.5 \mu\text{M}$ ,  $[\text{CO}_3]_{\text{T}} = 10 \text{ mM}$ , Temperature =  $25 \text{ }^\circ\text{C}$ , and  $[\text{HOCl}]_{\text{T}} = 10, 50, 100 \mu\text{M}$ . 95% confidence intervals about the regression line shown.

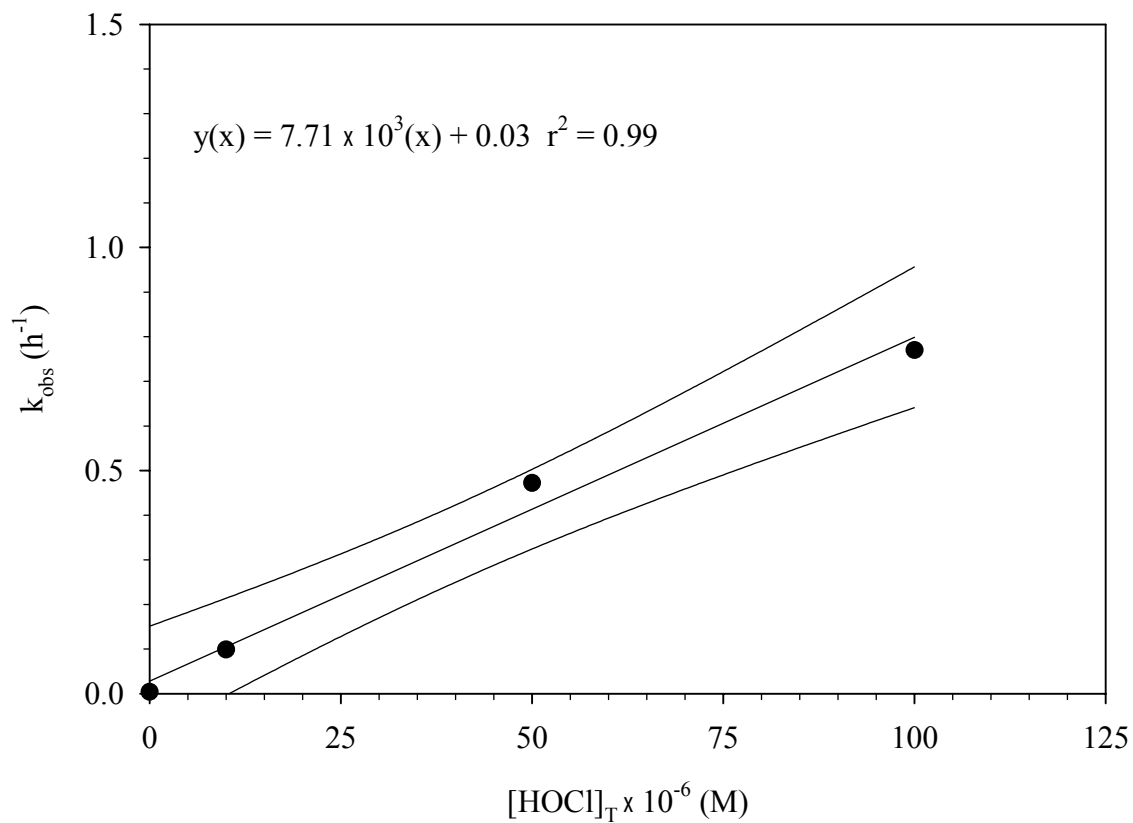


Figure 21 Apparent second order reaction rate coefficient for CP in the presence of free chlorine at pH 10.  $[\text{CP}]_0 = 0.5 \mu\text{M}$ ,  $[\text{CO}_3]_{\text{T}} = 10 \text{ mM}$ , Temperature =  $25 \text{ }^\circ\text{C}$ , and  $[\text{HOCl}]_{\text{T}} = 10, 50, 100 \mu\text{M}$ . 95% confidence intervals about the regression line shown.



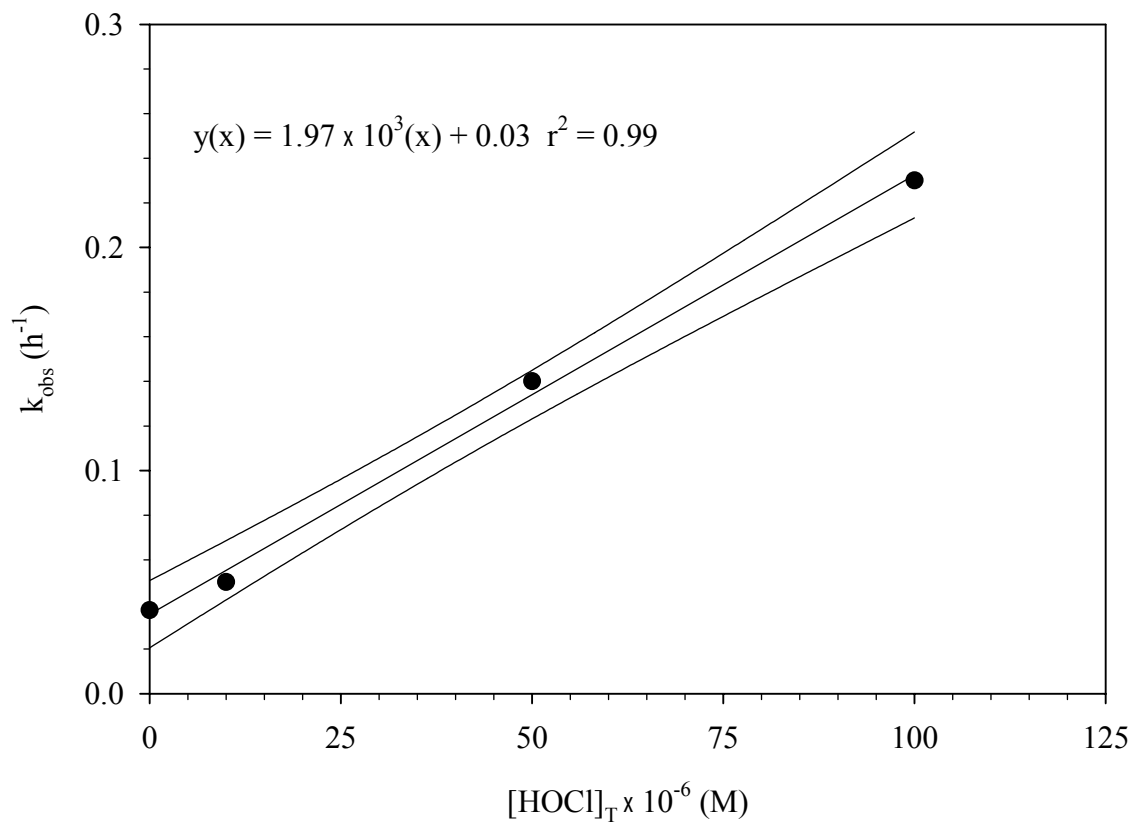


Figure 22 Apparent second order reaction rate coefficient for CP in the presence of free chlorine at pH 11.  $[\text{CP}]_0 = 0.5 \mu\text{M}$ ,  $[\text{CO}_3]_{\text{T}} = 10 \text{ mM}$ , Temperature =  $25 \text{ }^\circ\text{C}$ , and  $[\text{HOCl}]_{\text{T}} = 10, 50, 100 \mu\text{M}$ . 95% confidence intervals about the regression line shown.

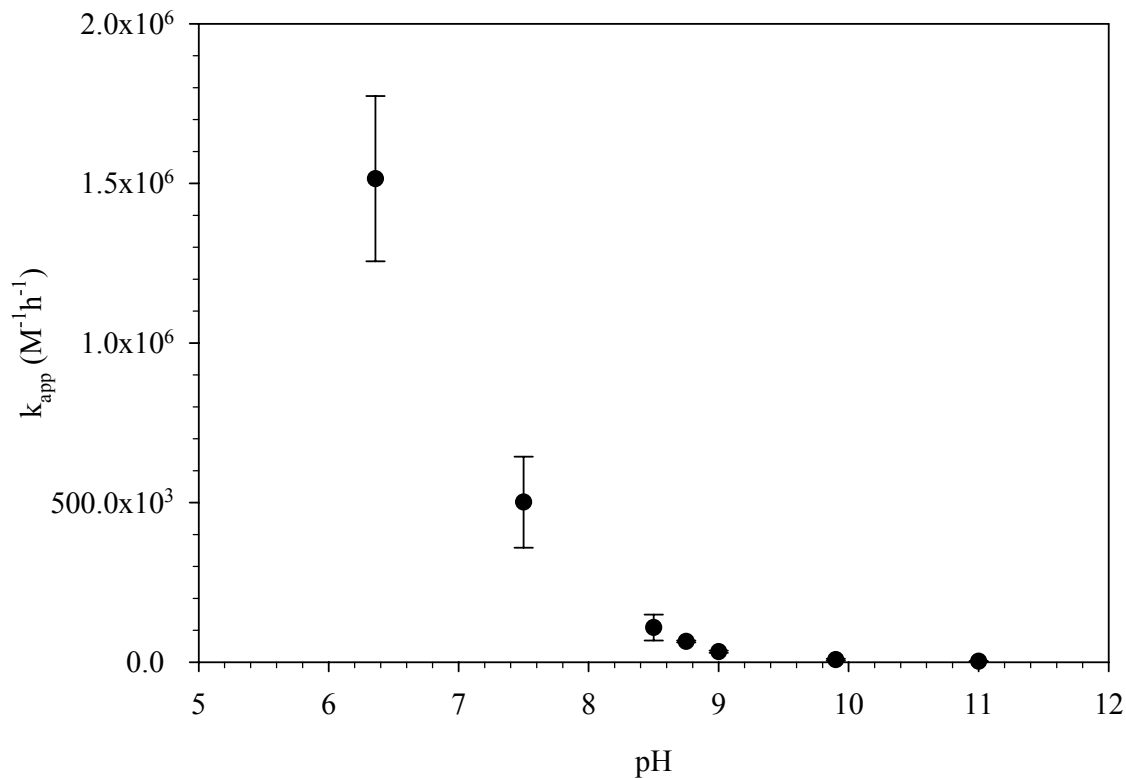


Figure 23 The pH dependence of the apparent second order rate constant for the reaction of free chlorine with CP.  $[CP]_0 = 0.5 \mu M$ ,  $[Buffer]_T = 10 \text{ mM}$ , Temperature =  $25 \pm 1^\circ C$ , and  $[HOCl]_T = 10, 50, \text{ and } 100 \mu M$ . Error bars represent 95% confidence intervals.

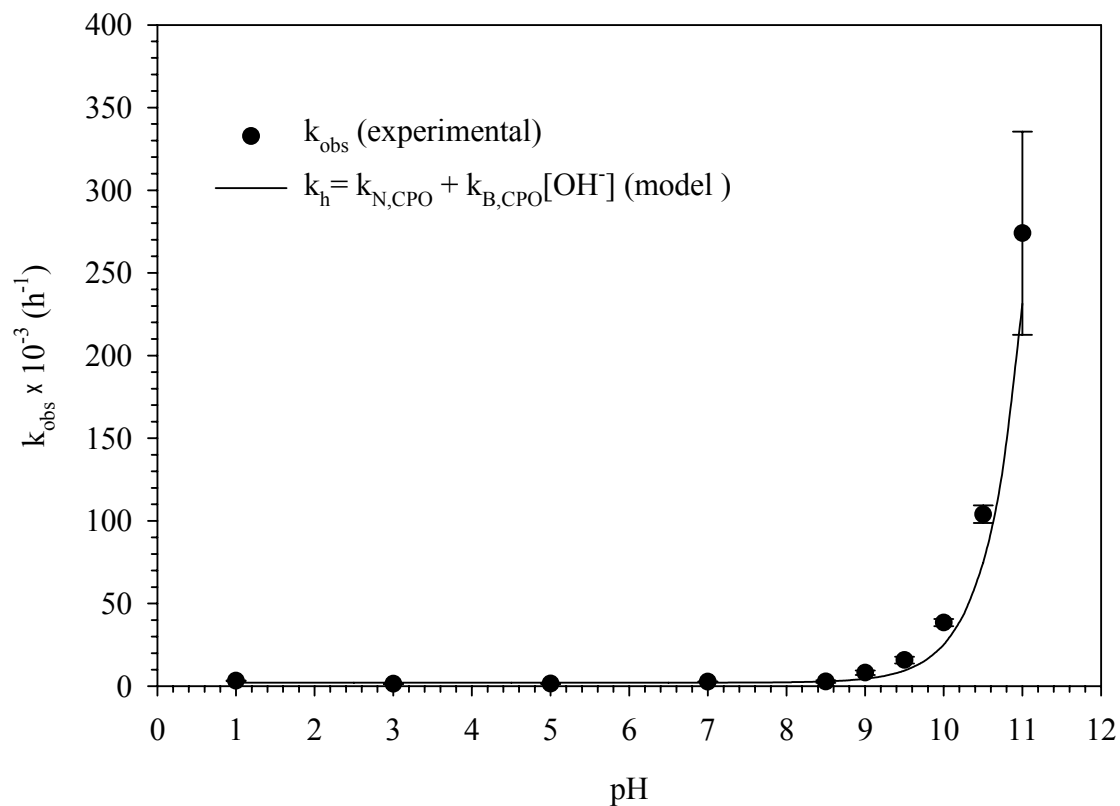


Figure 24 Experimental and model predictions for the first order observed hydrolysis of CPO over the pH range of 1-11.  $[\text{CPO}]_0 = 0.5 \mu\text{M}$ ,  $[\text{Buffer}]_T = 10 \text{ mM}$ , and Temperature =  $25 \pm 1^\circ\text{C}$ . Error bars represent 95% confidence intervals and the line represents model results.

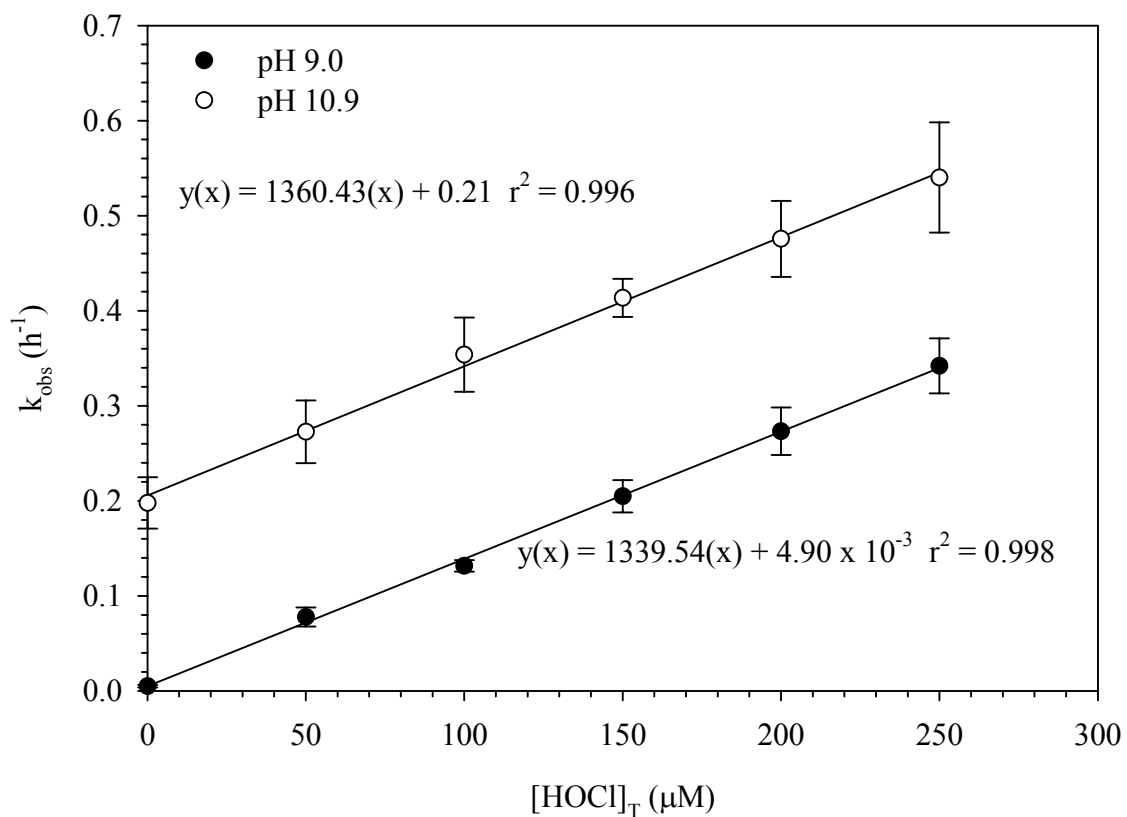


Figure 25 Second order rate coefficient for chlorine assisted hydrolysis of CPO at pH 9 and 10.9.  $[CPO]_0 = 0.5 \mu\text{M}$ ,  $[CO_3]_T = 10 \text{ mM}$ , Temperature =  $25 \pm 1^\circ\text{C}$ , and  $[HOCl]_T = 0 - 250 \mu\text{M}$ . Error bars represent 95% confidence intervals.

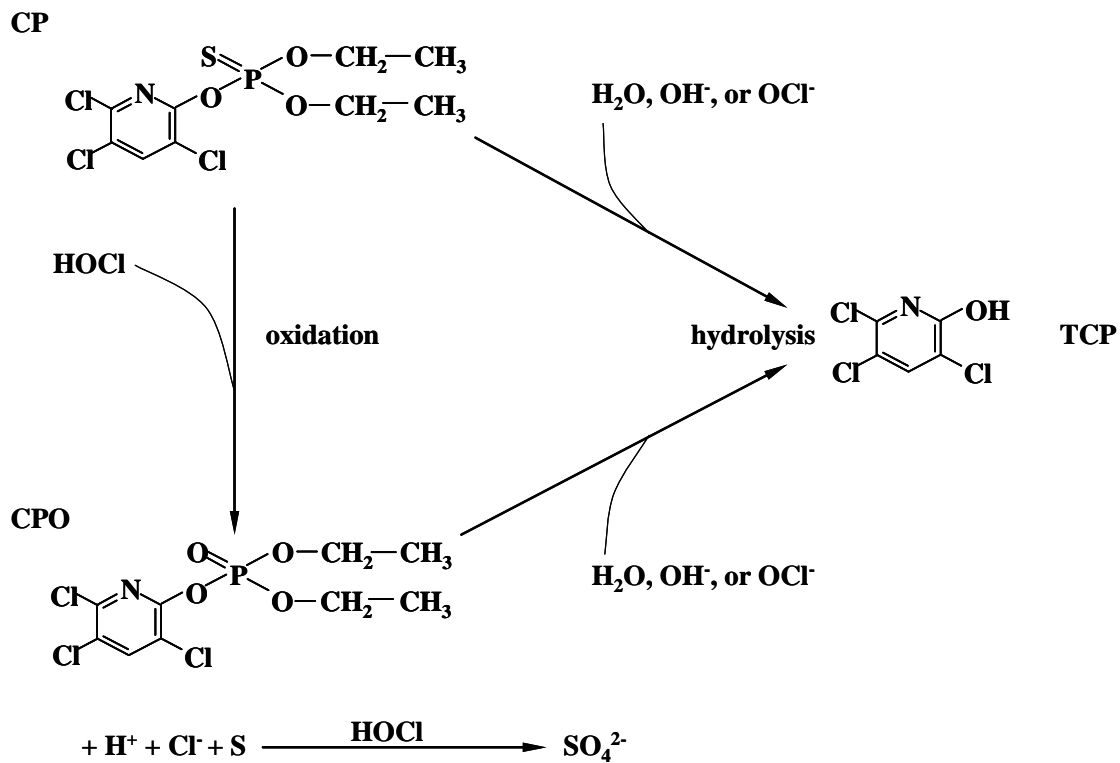


Figure 26 Simplified schematic of chlorpyrifos degradation pathways in the presence of chlorine at near neutral and alkaline pH.

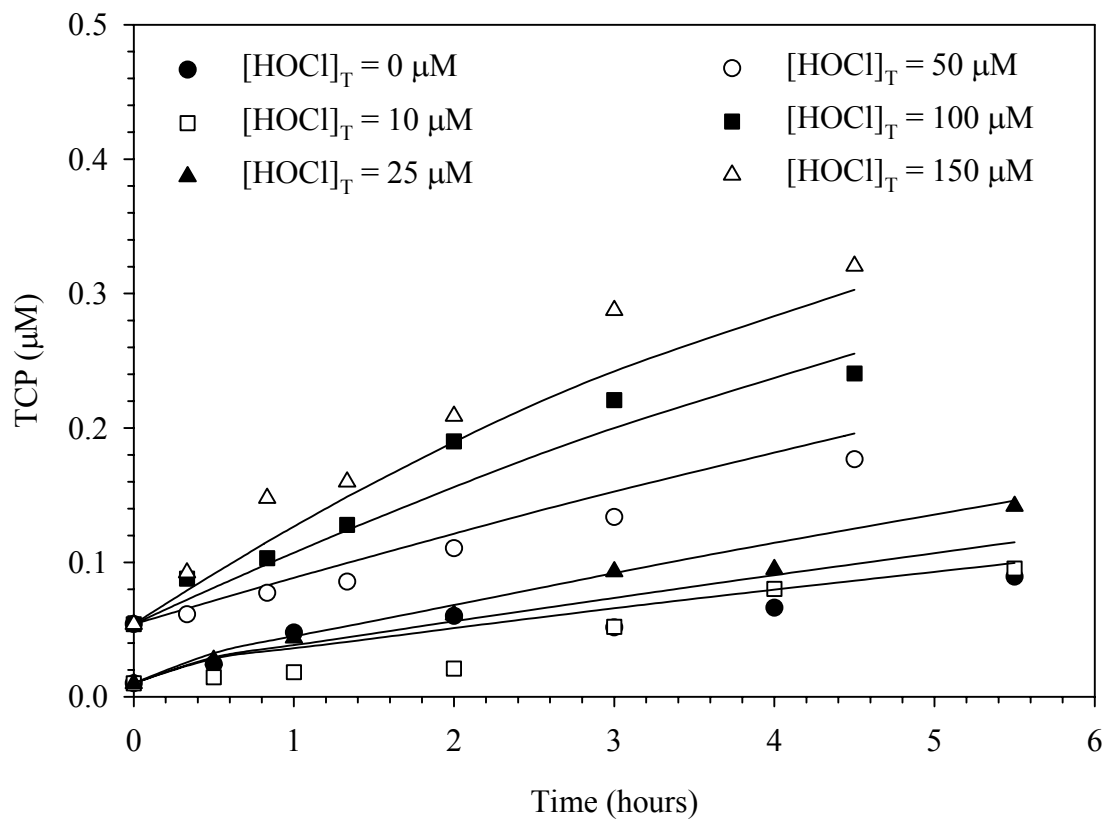


Figure 27 TCP experimental and model results for the loss of CP in the presence of free chlorine at pH 11 .  $[CP]_0 = 0.35 \mu\text{M}$ ,  $[\text{CO}_3]_T = 10 \text{ mM}$ , Temperature =  $25 \pm 1^\circ\text{C}$ , and  $[\text{HOCl}]_T = 0 - 150 \mu\text{M}$ . Lines represent model results.

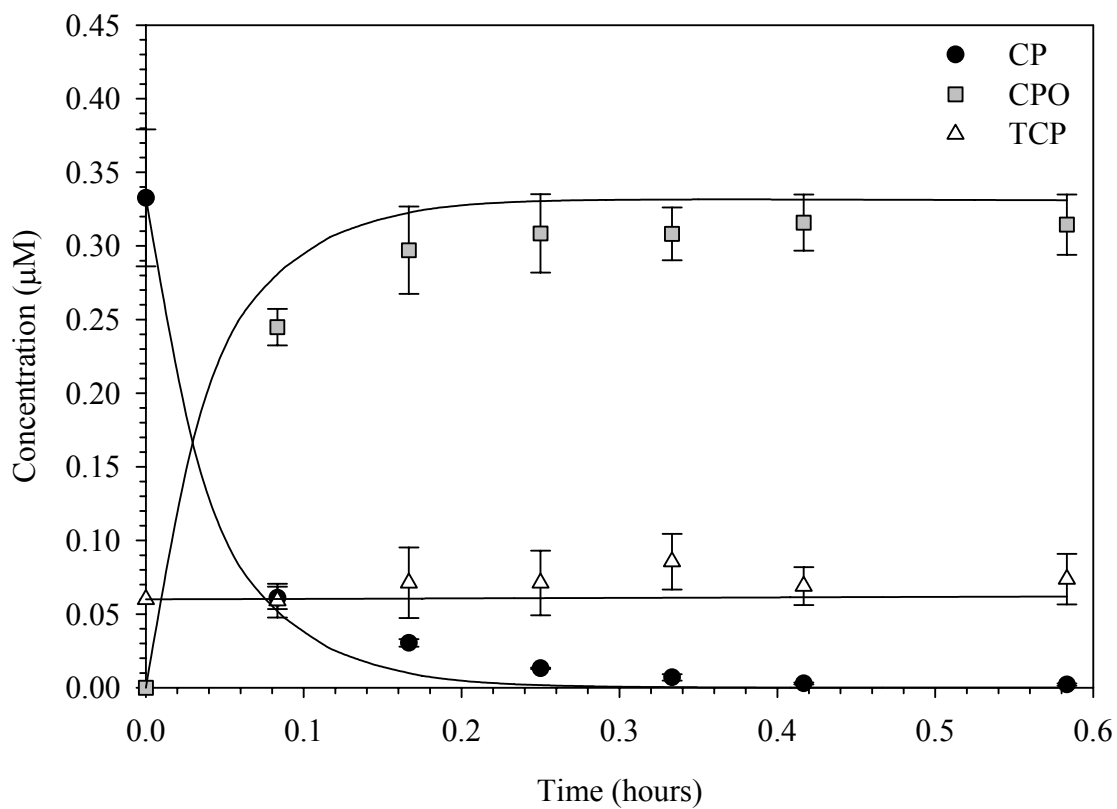


Figure 28 CP degradation in the presence of free chlorine at pH 7.15.  $[CP]_0 = 0.33 \mu\text{M}$ ,  $[\text{CO}_3]_{\text{T}} = 1 \text{ mM}$ , Temperature =  $25 \pm 1^\circ\text{C}$ , and  $[\text{HOCl}]_{\text{T}} = 20 \mu\text{M}$ . Lines represent model results and error bars are 95% confidence intervals.

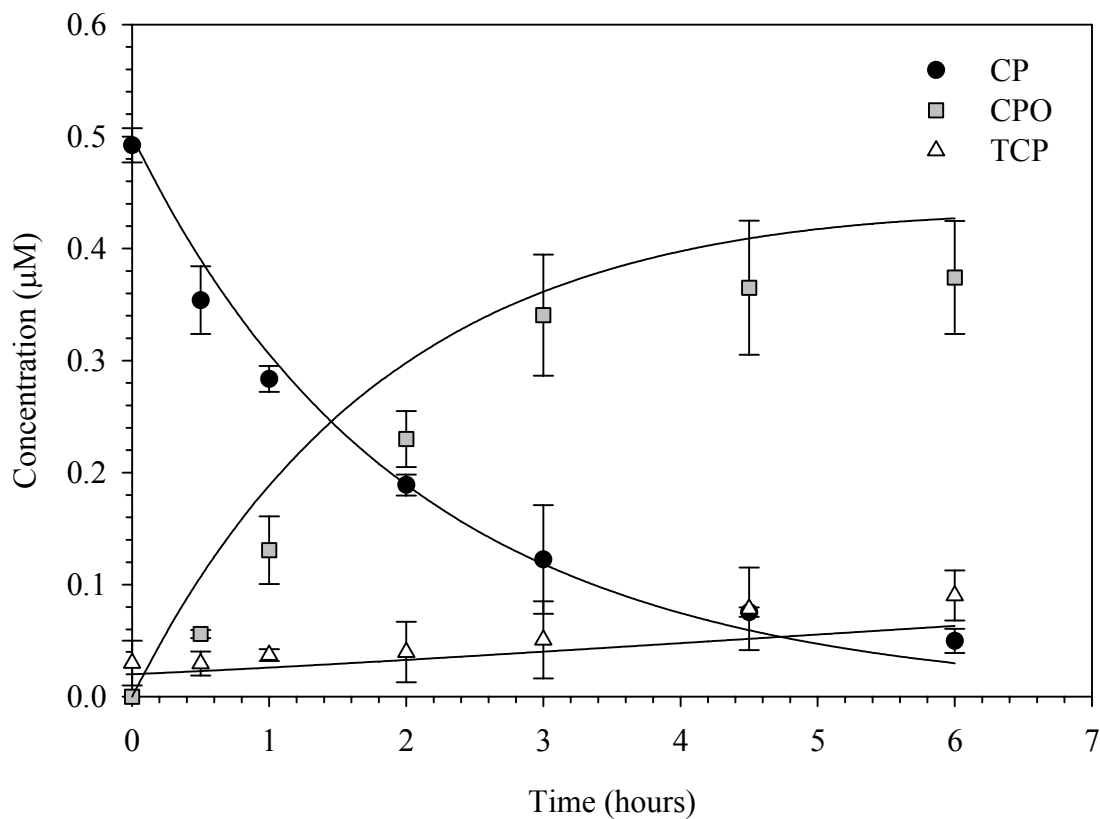


Figure 29 CP degradation in the presence of free chlorine at pH 9.0.  $[CP]_0 = 0.5 \mu\text{M}$ ,  $[\text{CO}_3]_T = 1 \text{ mM}$ , Temperature =  $25 \pm 1^\circ\text{C}$ , and  $[\text{HOCl}]_T = 10 \mu\text{M}$ . Lines represent model results and error bars are 95% confidence intervals.